

**TENSION STRENGTH OF EMBED PLATES WITH WELDED
DEFORMED BARS AS GOVERNED BY CONCRETE BREAKOUT**

by

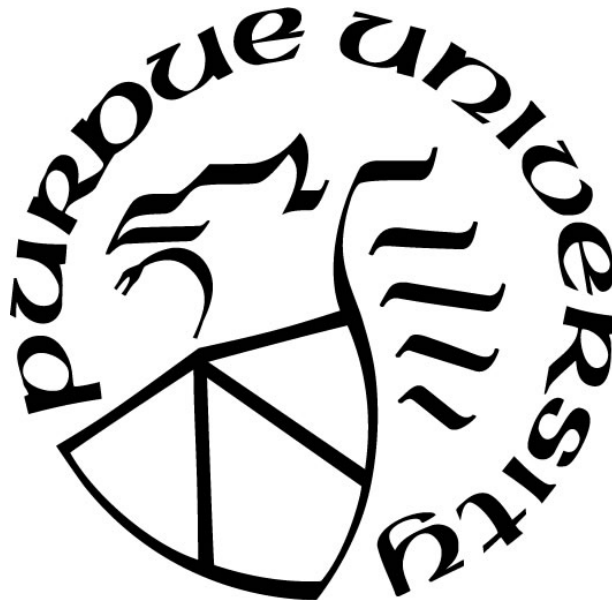
Ata Ur Rehman

A Thesis

Submitted to the Faculty of Purdue University

In Partial Fulfillment of the Requirements for the degree of

Master of Science in Civil Engineering



Lyles School of Civil Engineering

West Lafayette, Indiana

August 2020

THE PURDUE UNIVERSITY GRADUATE SCHOOL
STATEMENT OF COMMITTEE APPROVAL

Dr. Amit H. Varma

Lyles School of Civil Engineering

Dr. Christopher S. Williams

Lyles School of Civil Engineering

Dr. Jungil Seol

Lyles School of Civil Engineering

Approved by:

Dr. Dulcy M. Abraham

*To my beloved Mother, Father, Wife-Aneesa, and three beautiful sons Abdul Raheem, Abdul
Hadi and Abdul Haseeb for their support, love and prayers*

ACKNOWLEDGMENTS

At first, I would like to thank my advisor, Dr. Amit Varma who provided me the opportunity to work on this project and I extend my gratitude for his support, guidance and inspiration during the project. I would like to pay special regards to Dr Jungil Seol for teaching, guiding, and helping me throughout the project. I would like to thank my examining committee member, Dr. Christopher Williams for this valuable time, support and supervision.

The research would have not been possible without the support of research team at Bowen laboratory, specially the Research Engineer Bradt Thomas who professionally taught me how to conduct experiments on the laboratory floor. I would like to thank Ph.D. candidate Hassan Sagheer for his motivation, inspiration and encouragement since my arrival at Purdue. Lastly, I am grateful to the Ministry of Defense, Pakistan for funding my research and providing the opportunity to enhance my knowledge and skills.

TABLE OF CONTENTS

| | |
|---|----|
| LIST OF TABLES | 6 |
| LIST OF FIGURES | 7 |
| ABSTRACT | 9 |
| 1. INTRODUCTION | 10 |
| 2. RESEARCH BACKGROUND | 14 |
| 2.1 Types and Behavior of Anchors under Tension Loading | 14 |
| 2.2 Design of Anchors under Tension | 18 |
| 3. LITERATURE REVIEW | 23 |
| 3.1 Prior Research on Reinforcing Bars as Anchorages | 23 |
| 3.2 Development Length Concept per ACI 318-19 | 26 |
| 4. EXPERIMENTAL STUDY | 28 |
| 4.1 Development of Test Matrix and Specimen Details | 28 |
| 4.2 Test Setup and Loading Protocol | 34 |
| 4.3 Sensor Layout | 34 |
| 5. TEST RESULTS | 38 |
| 5.1 Test # 1 - 5x5 DRA # 5 | 39 |
| 5.2 Test # 2 - 5x5 DRA # 5 | 41 |
| 5.3 Test # 3 – 5x5 DWA 4/8 | 42 |
| 5.4 Test # 4 – 5x5 DWA 4/8 | 44 |
| 5.5 Test # 5 – 5x5 DWA 5/8 | 46 |
| 5.6 Test # 6 – 5x5 DWA 5/8 | 48 |
| 5.7 Test # 7 – 3x3 DWA 5/8 | 50 |
| 5.8 Test # 8 – 3x3 DWA 5/8 | 51 |
| 5.9 Summary of Test Results | 54 |
| 6. CONCLUSIONS AND FUTURE WORK | 55 |
| REFERENCES | 56 |
| APPENDIX A | 58 |
| APPENDIX B | 69 |
| APPENDIX C | 74 |

LIST OF TABLES

| | |
|--|----|
| Table 3.1 Various Methods for Designing Rebars as Anchorages | 26 |
| Table 4.1 Test matrix of grouped anchor tests..... | 32 |
| Table 4.2 Concrete block dimension of grouped anchor tests | 32 |
| Table 4.3 Expected failure modes of grouped anchor tests | 33 |
| Table 5.1 Summary of Test Results..... | 38 |

LIST OF FIGURES

| | |
|---|----|
| Figure 1.1 Anchorage assembly for (a) Reinforced Concrete walls, and (b) Steel plate Composite walls in safety-related structures, (redrawn from (Chicchi et al., 2020)) | 11 |
| Figure 2.1 Transfer Mechanism (a) Mechanical interlock (b), Frictional interlock and (c) Bond (redrawn from (Eligehausen, 2006))..... | 15 |
| Figure 2.2 Types of anchors (a) Cast-in headed stud anchor, (b) Post-installed undercut and (c) expansion anchors, and (d) Adhesive anchors (Taken from (P. Mahrenholtz & Eligehausen, 2015)) | 16 |
| Figure 2.3 Failure modes for anchors under tension (redrawn from ACI 318-19)..... | 17 |
| Figure 2.4 Idealized load-displacement curves for anchors under external tension loading (redrawn from (Eligehausen, 2006)) | 18 |
| Figure 2.5 Concrete breakout cone predicted by 45-degree cone model (redrawn from (Fuchs et al., 1995)) | 19 |
| Figure 2.6 Idealized section through concrete breakout cone (redrawn from ACI 318-19)..... | 20 |
| Figure 3.1 Group anchor assembly configuration (redrawn from Chicchi et al., 2020)..... | 24 |
| Figure 3.2 (a) Breakout cone and (b) Initiation of breakout cone from anchor base (picture from Chicchi et al., 2020) | 25 |
| Figure 4.1 Cross-section of concrete block for 3x3 DWA 5/8 specimen | 30 |
| Figure 4.2 Concrete breakout cone with the effect of post-tensioning forces | 31 |
| Figure 4.3 Test frame with the test specimen (Chicchi et al., 2020) | 34 |
| Figure 4.4 Sensor layout for grouped anchor specimens: (a) displacement transducers, (b) strain gages for test no 1,2,3 and 4 (c) strain gages for test 5 and 6 and (d) strain gages for test 7 and 8 | 36 |
| Figure 4.5 Linear variable displacement transducers (LVDTs, DT3 ~ DT6) installed on the concrete surface of the specimen | 37 |
| Figure 5.1 Applied force-displacement (P- Δ) response of Test 1 | 39 |
| Figure 5.2 Plan view of cracks formed on the concrete surface | 40 |
| Figure 5.3 Breakout cone with an average angle of 34.22 degrees | 40 |
| Figure 5.4 Applied force-displacement (P- Δ) response of Test 2..... | 41 |
| Figure 5.5 Plan view of cracks and formed on the concrete surface | 42 |
| Figure 5.6 Breakout cone with an average angle of 36.77 degrees | 42 |
| Figure 5.7 Applied force-displacement (P- Δ) response of test 3 | 43 |

| | |
|--|----|
| Figure 5.8 Plan view of cracks formed on the concrete surface | 44 |
| Figure 5.9 Breakout cone with average angle of 36.23 degrees | 44 |
| Figure 5.10 Applied force-displacement (P- Δ) response of test 4 | 45 |
| Figure 5.11 Plan view of cracks formed on concrete surface | 45 |
| Figure 5.12 Breakout cone with average angle of 30.15 degrees | 46 |
| Figure 5.13 Applied force-displacement (P- Δ) response of test 5 | 47 |
| Figure 5.14 Plan view of cracks and formed on the concrete surface | 47 |
| Figure 5.15 Breakout cone with average angle of 26.25 degrees | 48 |
| Figure 5.16 Applied force-displacement (P- Δ) response of test 6 | 49 |
| Figure 5.17 Plan view of cracks and formed on the concrete surface | 49 |
| Figure 5.18 Breakout cone with an average angle of 26.56 degrees | 50 |
| Figure 5.19 Applied force-displacement (P- Δ) response of test | 51 |
| Figure 5.20 (a) and (b) Illustrates Pull-out failure | 51 |
| Figure 5.21 Applied force-displacement (P- Δ) response of test 8 | 52 |
| Figure 5.22 Pulled out and Ruptured bars | 52 |
| Figure 5.23 Ruptured bars..... | 53 |
| Figure 5.24 Pulled out bars | 53 |

ABSTRACT

Embedded plates are used to support the external attachments such as heavy piping, brackets, sprinkler systems, or other equipment in nuclear power plants. The plates are welded with deformed reinforcing bars or deformed wires and anchored to reinforced concrete walls. The ACI code (ACI 318-19/ACI 349-13) provides design equations to calculate the anchor strength in concrete under tension load. These empirical equations are based on experiments conducted on headed studs, hooked bars, headed bolts, and adhesive anchors. With the lack of experimental data and code provisions on straight deformed reinforcing bars or deformed wires used as anchors, it is believed that anchoring bars with the embedment length as per code prescribed development length will provide sufficient strength to transfer tensile forces to the concrete, ignoring other failure modes such as concrete breakout.

In this study, eight large scale group anchor tests were performed to evaluate their concrete breakout strength as per ACI 349-13. The test specimens were made with deformed reinforcing bar anchors (DRAs) and deformed wire anchors (DWAs). The tests included the effect of different bar types, bar sizes, and anchor spacings on the breakout capacities of such connections. The mean average back-calculated effective k value is 33.25 for DRAs and 36.26 for DWAs. The experimental study confirms that the axial tension capacity of embedded plates anchored to concrete using deformed reinforcing bars or deformed wires can be limited by concrete breakout strength.

1. INTRODUCTION

Embedments are often used in safety-related nuclear facilities to provide attachment for equipment or to anchor components and piping. These facilities are constructed using massive concrete members, including thick reinforced concrete walls and steel-plate composite (SC) walls. According to ACI 349-13, the term “embedment” is used for a fabricated steel plate equipped with anchors or reinforcing bars embedded in the concrete surface. Such steel embed plates may employ deformed reinforcing bars anchors (DRAs conforming to, e.g., ASTM A706) or deformed wire anchors (DWAs conforming to ASTM A1064), either hooked, straight or headed, as the anchor elements. Here, the word “anchor” defines a bar welded to a steel plate. The thick concrete walls of the nuclear structures provide enough space (depth) for longer embedments. The non-structural attachments or piping are attached to the face of the embed steel plate, as shown in Figure 1.1(a). In SC walls, the anchor bars (DRA or DWA) are welded to the faceplate, whereas the other end is embedded in concrete, as shown in Figure 1.1(b). The steel plate provides means to attach external attachments generally via welding such as piping brackets, railings, sprinkler systems, etc. The steel plate and anchors (embedment) transfers the tensile forces to the concrete.

According to ACI 349-13, the bar length is determined using the provisions of full development length (l_d) concept of reinforcing bars regardless of bar spacing or edge distance. Except for bar yield or bar rupture, the development length provisions rule out other failure modes for such embedments. However, the splitting failure is directly addressed in the design of development length equations. Accordingly, no check for the concrete breakout is performed in the design of these embed plates. However, there is little to no experimental data available regarding the axial tension behavior and pullout strength of embed plates designed in this manner.

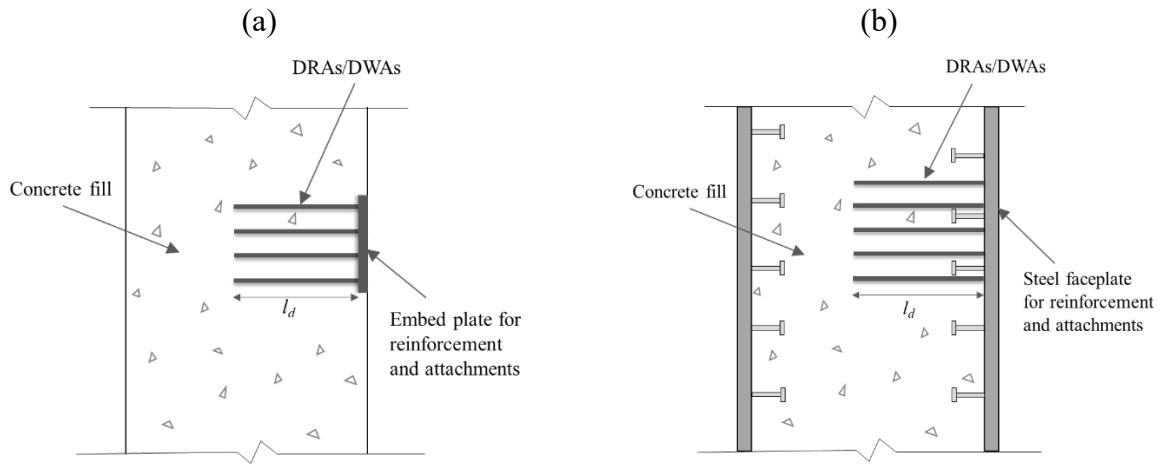


Figure 1.1 Anchorage assembly for (a) Reinforced Concrete walls, and (b) Steel plate Composite walls in safety-related structures, (redrawn from (Chicchi et al., 2020))

The absence of experimental data has led to the erroneous assumption that if the reinforcing bars are fully developed as per ACI 349-13 and ACI 318-19, then no further design checks are needed. However, regulators and code committees have raised the issue of whether concrete breakout failure modes should be considered in the design of such connections. The ACI 349 code is silent on checking concrete breakout failure mode for steel embed plates equipped with fully developed DRAs and DWAs. Particularly, there is very little experimental data available regarding the use of DRAs (deformed reinforcement bar anchors) and DWAs (deformed wire anchors) as anchors.

If, as recent testing (Chicchi et al., 2020) confirms, the axial tensile strength of embed plates equipped with welded reinforcing bars can be limited by concrete breakout strength (as opposed to bar yield or bar rupture), then the provisions for anchorage to concrete in ACI 349-13, which include checks for the concrete breakout, would apply. However, since these provisions often result in tension capacities significantly lower than those associated with bar yield and bar rupture, this alarms the design community. Then the question becomes, how to anticipate the failure mode associated with embed plates welded with DRAs and DWAs, and how to accurately estimate the breakout capacities using code provisions.

The objective of this study is to experimentally evaluate the applicability of the ACI 349-13 breakout design for embed plates with welded DRAs and DWAs and assess the effective k values in the breakout design equation. The research objective is achieved by (i) testing eight group anchor specimens, subjected to axial tension encompassing both DRA and DWA as anchors and (ii) recommending the design value associated with estimating the concrete breakout strength based on the experimental results

The research outline is as follows:

- Chapter 2: Research Background

This chapter presents a brief description of the development of the current design code provisions based on the concrete capacity design (CCD) method. It explains the various type of anchorage systems and the potential failure modes under tension loads. The effect of cracked and uncracked concrete on failure modes is also discussed. It also covers the concept of full development length and effective embedment length concepts provided by the code.

- Chapter 3: Literature Review

This chapter discusses the previously conducted research on conventional anchorages in concrete. Studies (Chicchi et al., 2017, 2020; Eligehausen, 2006; Eligehausen & Sawade, 1989; Fuchs et al., 1995; C. Mahrenholtz et al., 2020) on the behavior of anchorages under tension are briefly discussed. It also explains the experimental studies conducted on the design and use of tension-loaded reinforcing bars as anchors.

- Chapter 4: Experimental Program

This chapter discusses the experimental program. It includes the development of the test matrix, design of experimental setup, geometry of specimens, loading protocols, and sensor layout.

- Chapter 5: Test Results

This chapter covers the results of the eight group anchor specimens, including load-displacement response, breakout cone angles, and back-calculated effective k -factor values.

- Chapter 6: Summary and Conclusion

This chapter enlists the summary of eight group anchor test results along with the analyses of the test results and essential conclusions. It also includes the limitation of the study and the scope of future research.

2. RESEARCH BACKGROUND

This chapter incorporates the review of research work in the field of anchorages. It includes current design provisions, type of anchorages, potential failure modes, and the effect of cracked and uncracked concrete on failure modes with an overview of the development length concept.

2.1 Types and Behavior of Anchors under Tension Loading

Various types of anchorages are developed and designed to attach structural or non-structural components to reinforced concrete structures. For the design of anchors in safety-related structures, the serviceability and ultimate limit state requirements shall be met. Code Requirements for Nuclear Safety-Related Concrete Structures and Commentary (ACI 349-13) provides basic models for the design of anchors in nuclear safety-related structures. ACI 318-19 also provides basic design equations to determine the strength of anchors with relevant failure modes. Anchors are broadly classified as cast-in anchors and post-installed anchors. Their function and mechanism are discussed in subsequent sections with a focus on cast-in and post-installed anchors.

Anchors behave differently under tension, shear, and combined loading. The discussion here is limited to anchors under tension loading only. Anchors transfer the tension load to the base in different ways. Typically, the load transfer mechanism for various anchors is through mechanical interlock, friction interlock, and bond (between adhesive and concrete or adhesive and anchor). The illustration of the load transfer mechanism is shown in Figure 2.1. For most cast-in anchors and few post-installed (undercut) anchors, the load is transferred via mechanical interlock. It transfers the applied load by providing a bearing interlock between anchor and concrete base. This mechanism is common in headed studs, anchor bolts, and hooked anchors. For post-installed expansion anchors, the external load is transferred via frictional interlock. The initiation of expansion forces at the base creates frictional interlock between the anchor and the concrete. Whereas, the chemical bond transfers the applied tension load through adhesion bond. All anchors exhibit one or the combination of the above load-transfer mechanisms.

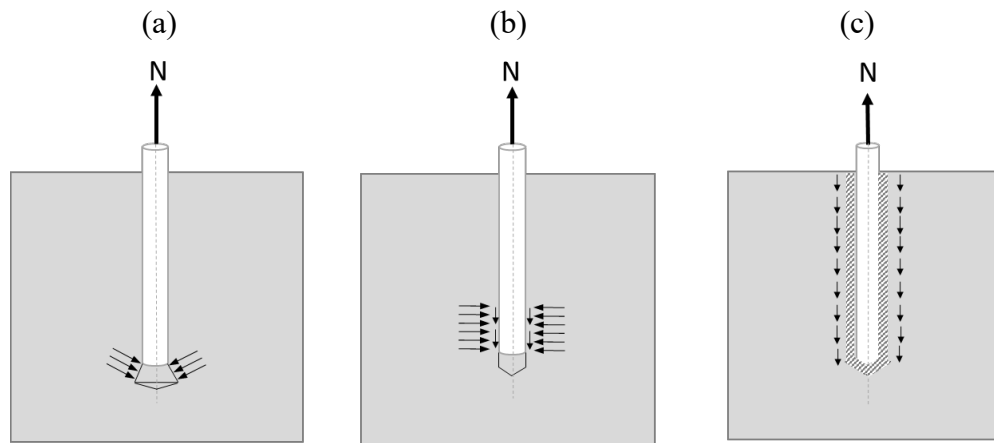


Figure 2.1 Transfer Mechanism (a) Mechanical interlock (b), Frictional interlock and (c) Bond (redrawn from (Eligehausen, 2006))

Cast-in anchors are attached to the formwork prior to the casting of the concrete. Their advantage lies in the known location of the external load, so the design of reinforced concrete members can be reinforced using appropriate reinforcement. Their disadvantage lies in the arrangement and potential for the wrong placement of anchors. Figure 2.2(a) illustrates a cast-in anchor, which may consist of a headed stud or headed bolt. The post-installed anchors are installed in hardened concrete via various drilling techniques (e.g., rotary impact drill, diamond core drill, rock drill, etc.). They are becoming very popular because of their flexibility and portability. The design strength is directly dependent upon the quality of the installation process. There are two sub-categories of post-installed anchors: mechanical (expansion) and bonded (adhesive) anchors. Figure 2.2(b), (c) and (d) shows post-installed undercut, expansion and adhesive anchors respectively.

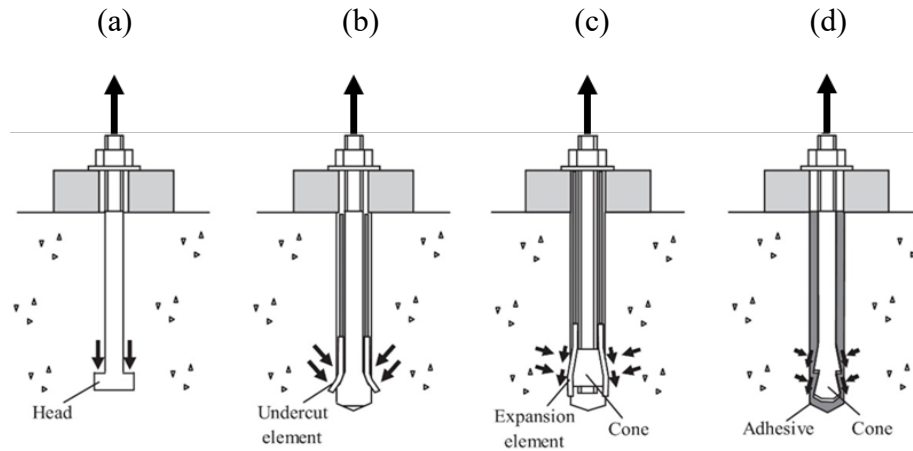


Figure 2.2 Types of anchors (a) Cast-in headed stud anchor, (b) Post-installed undercut and (c) expansion anchors, and (d) Adhesive anchors (Taken from (P. Mahrenholtz & Eligehausen, 2015))

The thesis focusses only on design and use of reinforcing bars and wires (DRAs or DWAs) as anchors, by considering them as cast-in anchors.

Figure 2.3 shows different failure modes of anchors subjected to tension load: (a) steel failure, (b) pullout, (c) concrete breakout, (d) bond failure, and (e) concrete splitting. The steel failure occurs when the steel material is sufficiently ductile, and has enough embedment length, so that anchor develops its yielding or ultimate tensile strength before concrete fails. The relative load-displacement curve is shown in Figure 2.4; considering the curve (a) for steel failure, the anchor has a longer embedment length than other anchors represented by curves (b), (c), and (d). Curve (b) represents pullout failure, which is the debonding (pulling out) of the anchor from the concrete base. This occurs in cast-in anchors if the anchor head or the bearing surface is inadequate. Pull-out is a common failure mode in deformation-controlled anchors (Eligehausen & Tamas Balogh, 1995). The load-displacement curve (c) in Figure 2.4 represents a concrete breakout failure, and curve (d) represents a concrete splitting .

Brittle failures are associated with the concrete breakout or concrete splitting failure modes. Splitting failure occurs in post-installed anchors with a relatively thin concrete member, and when

anchors are placed close to an edge or a group of anchors are installed very close to each other (less than the critical spacing specified in ACI 318-19). Many anchors are designed to reach their concrete breakout capacity before reaching yield or rupture (ultimate) strength. Details of the breakout design method are discussed in the next section (Section 2.2: Design of anchors under tension).

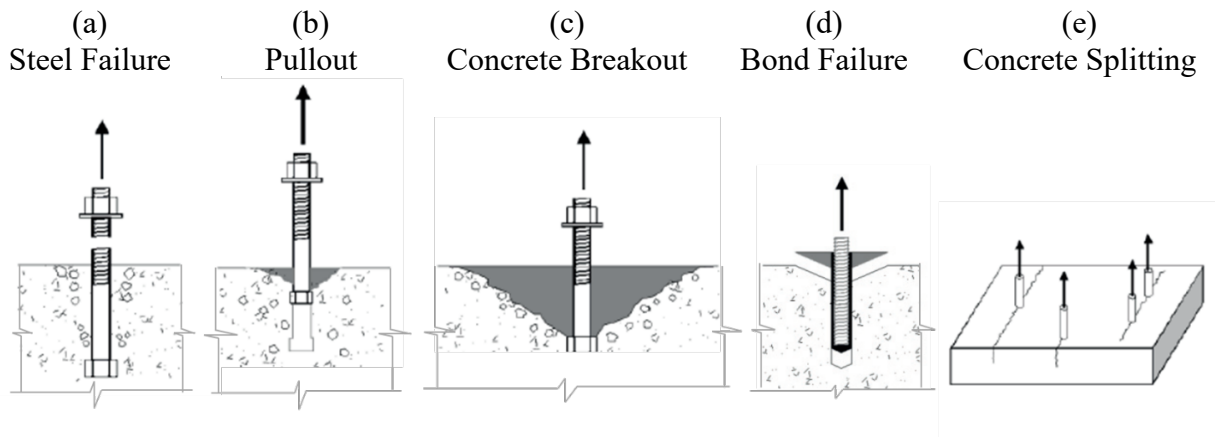


Figure 2.3 Failure modes for anchors under tension (redrawn from ACI 318-19)

Adhesive anchors are steel anchors inserted in drilled hole in hardened concrete with some adhesive (bonding material). The nominal strength of these anchors depends upon the mean bond strength of the anchor, specified by the manufacturer along with the installation technique. The product standards and qualifications are provided in ACI 355.4-19 (ACI Committee 355, 2019b). The design of post-installed bonded anchors is also briefly discussed in the subsequent section.

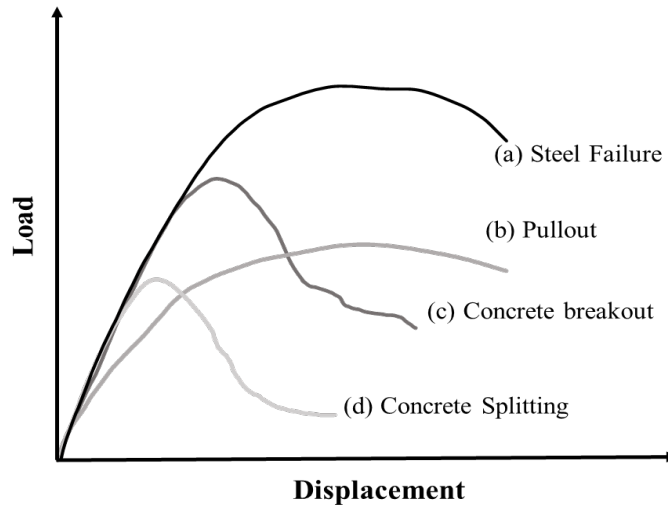


Figure 2.4 Idealized load-displacement curves for anchors under external tension loading (redrawn from (Eligehausen, 2006))

2.2 Design of Anchors under Tension

Anchors loaded in tension in concrete often fail by pulling a breakout cone from the concrete base, provided the steel strength of the anchors is not reached and anchors are far away from the edge. Previous research has shown that anchors under tension load develop circumferential stresses around the anchor zone (Eligehausen, 2006). Small micro-cracks are initiated even at low service level loads (30% of the ultimate load). The cracks propagate from the bottom of the anchor to the top concrete surface with an increase in applied load. The angle of the breakout cone relative to the concrete surface typically varies between 30 to 40 degrees. The ACI 349-85 (45-degree cone model) and Concrete Capacity Design (Fuchs et al., 1995) (CCD, 35-degree cone model) are the approaches used to calculate the breakout capacity of anchors in concrete. The models assume that the failure load depends upon the tensile capacity of the concrete.

The first model explaining the breakout behavior called the 45-degree cone model was introduced in ACI 349-85. Because of extra safety in nuclear-related structures, the ACI 349 committee wanted to avoid brittle concrete failure and design the anchors as ductile steel members. This concrete cone model assumes the constant tensile stress of $4\sqrt{f'_c}$ psi acting over the projected

failure area at an angle of 45 degrees. Figure 2.5 shows the projected failure area of a single anchor under tension load, making a cone at an angle of 45 degrees between the failure surface and the concrete surface.

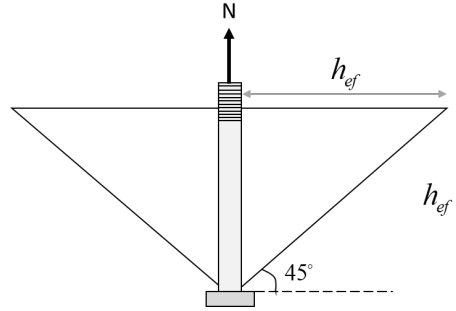


Figure 2.5 Concrete breakout cone predicted by 45-degree cone model (redrawn from (Fuchs et al., 1995))

The breakout capacity of a single anchor using this model is calculated from Eq (2) as below:

$$N_{no} = 4\sqrt{f'_c} \cdot \pi \cdot (A_{No}) \quad \text{Eq 1(a)}$$

$$A_{No} = \pi \cdot h_{ef}^2 \cdot \left(1 + \frac{d_u}{h_{ef}}\right) \quad \text{Eq 1(b)}$$

$$N_{no} = 4\sqrt{f'_c} \cdot \pi \cdot h_{ef}^2 \cdot \left(1 + \frac{d_u}{h_{ef}}\right) \quad \text{Eq 2}$$

Here N_{no} is the mean concrete breakout failure load of a single anchor, A_{No} in Eq (1 (a)) and Eq (1 (b)) is the projected failure area of a single anchor, f'_c is the compressive strength of the concrete, h_{ef} is the embedment depth of the anchor inside the concrete and d_u is the anchor diameter. The two studies (Bazant & Asce, n.d.) and (Fuchs et al., 1995) concluded that the results from this model overestimate the concrete cone capacity because it assumes constant tensile stress over the projected failure area and neglects the size effect.

The most authenticated model to calculate the concrete breakout capacity is the CCD (Concrete Capacity Design) (Fuchs et al., 1995) model. It assumes a 35-degree breakout cone and incorporates the size effect and edge effect in determining anchor capacity. The idealized projected failure area is considered to be a pyramid with the horizontal extent of three times the effective embedment depth ($3 h_{ef}$) as shown in Figure 2.6.

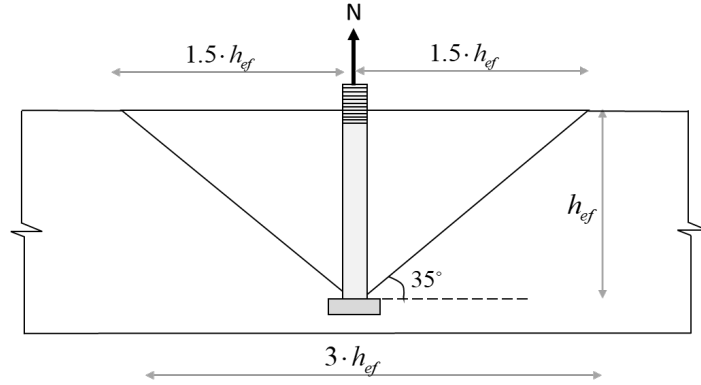


Figure 2.6 Idealized section through concrete breakout cone (redrawn from ACI 318-19)

The nominal concrete breakout capacity of a single anchor in tension unaffected by edge effects and neighboring anchors in uncracked concrete is given by Eq (2) ((Fuchs et al., 1995)

$$N_{no} = k_{nc} \cdot \sqrt{f'_c} \cdot h_{ef}^{1.5} \quad \text{Eq 3}$$

Eq (3) is an empirical equation, where N_{no} is the mean concrete breakout failure load of a single anchor, k_{nc} is the empirical constant, h_{ef} is the effective embedment depth of the anchor inside the concrete, and f'_c is the compressive strength of the concrete. The constant k_{nc} is calculated from a significant number of tests performed by (Fuchs et al., 1995). The model was approved and introduced in ACI 318 and ACI 349 codes, and it is still part of the latest ACI 318-19 and ACI 349-13 code versions. The advantage of the CCD model is that it also caters for the edge effect, critical spacing, group effects, and the effect of cracked and uncracked concrete.

After considering all the above factors, ACI 318-19 provides the nominal concrete breakout strength of a single and group of anchors in tension in cracked concrete, given by Eq (4) and Eq (5) respectively:

$$N_{cb} = \frac{A_{nc}}{A_{nco}} \cdot \psi_{ed,n} \cdot \psi_{c,n} \cdot \psi_{cpn} \cdot N_b \quad \text{Eq 4}$$

$$N_{cbg} = \frac{A_{nc}}{A_{nco}} \cdot \psi_{ec,n} \cdot \psi_{ed,n} \cdot \psi_{c,n} \cdot \psi_{cpn} \cdot N_b \quad \text{Eq 5}$$

Where the basic concrete breakout strength, N_b of a single anchor, is given by Eq (6):

$$N_b = k_c \cdot \lambda \cdot \sqrt{f'_c} \cdot h_{ef}^{1.5} \quad \text{Eq 6}$$

Here, A_{nc} is the total projected failure area of a single or group of anchors, calculated from the base of the exterior anchor projecting the failure surface 1.5 times h_{ef} , A_{nco} is the total projected failure area of a single anchor, and shall be calculated by:

$$A_{nco} = 9 \cdot h_{ef}^2 \quad \text{Eq 7}$$

In Eq (4) and Eq (5), $\psi_{ec,N}$, $\psi_{ed,N}$, $\psi_{c,N}$, $\psi_{cp,N}$ are the eccentricity, edge effect, cracking, and splitting factors, respectively. These factors are not discussed in detail here as they are not involved in the research study described in this thesis except the factor for uncracked concrete (i.e., $\psi_{cp,N} = 1.4$ for uncracked concrete). The factor A_{nc}/A_{nco} is the modification factor that considers the effect of multiple (group) anchors and the spacing of anchors on concrete breakout capacity under tension load.

The factor k_c in Eq (6) is an empirical constant derived from a large database of tests performed by (Fuchs et al., 1995) in uncracked concrete. The influence of the so-called size effect is integrated into the k_c factor. In ACI 318-19 code, the default value of k_c is 24 for cast-in anchors and 17 for

post-installed anchors for cracked concrete. The conversion factors for cast-in anchors and post-installed anchors from cracked to uncracked concrete conditions are 1.25 and 1.4, respectively. In ACI 349 and ACI 318, the design equations are typically calibrated with 90% confidence to stipulate a prediction of the 5% fractile strength. Conservatively, the ratio of nominal to the mean value is assumed to be 0.75. With a 95% probability, this relates to a ratio of 5% fractile to a mean of 0.75. The reported mean values of k_c from breakout tests in uncracked concrete are 40 ($24 \times 4/3 \times 1.25 = 40$) for cast-in anchors and 35 ($17 \times 4/3 \times 1.4 = 31.7$) for post-installed anchors. The value of k_c for adhesive anchors is approximately equal to the k_c value of post-installed expansion anchors (i.e., $k_c = 35$). However, k_c for post-installed anchors shall be adjusted as per product-specific tests based on ACI 355.2 (ACI Committee 355, 2019a) and ACI 355.4 (ACI Committee 355, 2019b).

The effects of cracking caused by external loads, intrinsic deformations (e.g., creep, shrinkage), and extrinsic deformations (e.g., temperature and support variations) are explained by (Nilforoush, 2017). The shape of the breakout cone is similar in uncracked and cracked concrete (Eligehausen & Ozbolt, n.d.). The anchor situated in cracked concrete reduces the breakout capacity by 25 percent (cast-in anchors). The reduction in capacity is due to the disturbance in the stress state around the anchor induced by the crack. However, reduction in adhesive anchor capacity is even more severe as the crack destroys the bond between the adhesive and concrete. Therefore, the cracking factor ($\psi_{c,N}$) is incorporated in design equations for determining breakout capacities in uncracked concrete. In the research detailed in this thesis, reinforced concrete is considered as uncracked (controlled environment).

3. LITERATURE REVIEW

This chapter discusses the previously conducted research on the behavior of reinforcing bars as anchorages in concrete structures and experimental studies focused on the design and the use of reinforcing bars as anchorages.

3.1 Prior Research on Reinforcing Bars as Anchorages

Over the past few years, several experimental and theoretical studies have been conducted to evaluate the behavior and design of rebars used as anchors (Chicchi et al., 2017), (C. Mahrenholtz et al., 2015), (C. Mahrenholtz et al., 2020), and (Chicchi et al., 2020). These studies include the design and qualification of reinforcing bars as anchors. According to (Chicchi et al., 2017), the breakout failure mode shall be considered in designing attachments to safety-related nuclear structures. In these structures, DRAs and DWAs welded to a steel plate embed in concrete are typically used as attachments. The DRAs and DWAs provide adequate strength to transfer tensile forces to the concrete if fully developed as per the ACI code. However, the question was raised regarding the possibility of other tension failure modes: a) concrete breakout, b) pullout, and c) weld rupture. The tests conducted by (Chicchi et al., 2020) are discussed and analyzed in detail in subsequent paragraphs.

The experimental testing of such connections (steel plate welded with DRAs/DWAs embedded in concrete) under tension load has been conducted by (Chicchi et al., 2020). The single anchor and group anchor tests were performed to validate the applicability of current breakout equations and appropriate failure modes. Thirteen single anchor (#6 and #9 DRA, and D-41.3 DWA) tests were conducted to understand bond behavior and the relationship between bond stress and slip. The observed bond stress of the anchors considering the uniform bond model is 119 psi (#6 DRA), 1,084 psi (#9 DRA), and 639 psi (D41.3 DWA). The specimen failed in pullout if the embedment length of the bar was less than the ACI 318 / ACI 349 specified development length. Generally, the steel failure was observed for the DRAs whose embedment lengths are equal or greater than the code specified lengths. However, pullout failure was observed for DWAs even when the embedment lengths were equal or greater than the code specified development lengths. This

pullout failure occurred due to the low bond strength of DWAs. Additionally, the development length equations in the codes apply only to DRAs.

The group anchor tests of straight and hooked bar configurations were performed to verify and analyze the design and behavior of group anchor assemblies under tension load. The eight group anchor specimens (5x5 #6 DRAs, 5x5 D-41.3 DWAs, 5x5 D-10.4 DWAs, 2x2 #9 hooked DRAs, and 4x4 D-10.4 hooked DWAs) with varying spacing were tested. The anchor assembly and configuration are shown in Figure 3.1. The effective embedment length (depth) (h_{ef}) is the embedment length (l_{emb}) of the bar plus the thickness of the plate. The expected breakout strengths were calculated using Eq. (5), Eq. (6) and Eq. (7) with $k_c = 31.7$ (used for post-installed anchors in ACI 349 code). The tensile strength of the connection is calculated by Eq. 8.

$$N = n \cdot A_b \cdot f_y \quad \text{Eq 8}$$

Here, n is the number of DWA/DRA bars welded to the embed plate, A_b is the area of the anchor and f_y is the yield strength of the bars.

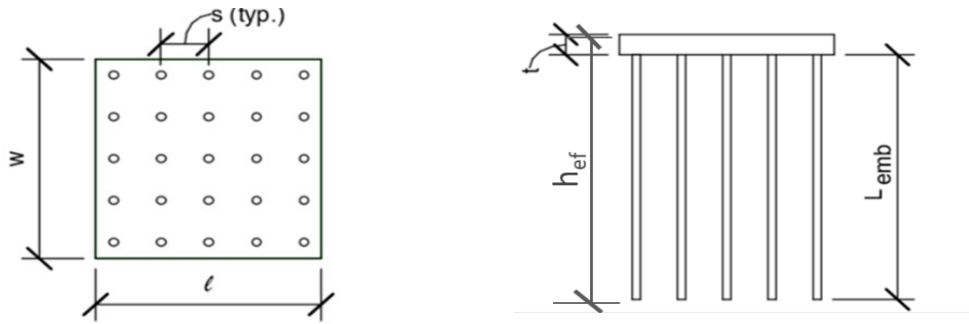


Figure 3.1 Group anchor assembly configuration (redrawn from Chicchi et al., 2020)

All group anchor specimens failed in breakout with failure load far below than yield or rupture strength of the welded anchor bars. The back-calculated k_{eff} value was determined using breakout Eq. (6). It is noted that the average back-calculated k_{eff} value for 5x5 #6 DRA specimens is 35.4,

and for 5x5 D-41.3 DWA specimens, it is 31.4. Figure 3.2 shows the breakout cone angle and the initiation point of the concrete breakout cone for the 5x5 D-41.3 DWA specimen. The breakout cone angle varies from 21 degrees to 45 degrees, as compared to the code (ACI 318) specified angle of 35 degrees. For the DWA specimen, the initiation of the failure plane starts at approximately 4 in. from the corner anchors and 2 in. from the edge anchors (Figure 3.2). On the contrary, for the DRA specimens, the concrete failure cone starts 1 in. from the base of the anchors. This effect is due to the reduced bond strength of the DWAs.

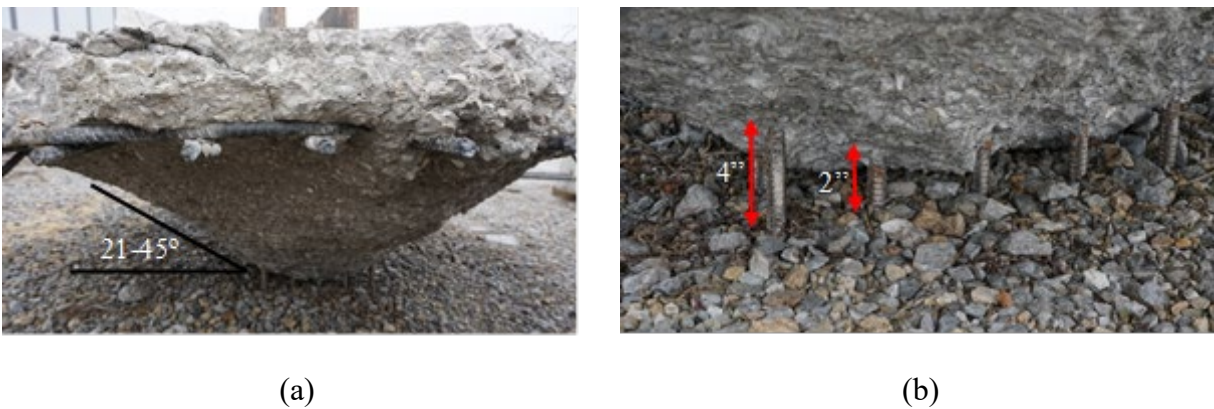


Figure 3.2 (a) Breakout cone and (b) Initiation of breakout cone from anchor base (picture from Chicchi et al., 2020)

The design of steel plates with welded reinforcing bars can be performed using the provisions of adhesive (bonded) anchors as per (Eligehausen, 2006). Recently, (C. Mahrenholtz et al., 2020) examined the qualification and design procedure for cast-in-place reinforcing bars by two methods, i.e., as an end-anchorage and as adhesive anchors. So currently there are three methods for design of rebars as anchorages as mentioned in Table 3.1. Which explains the design equations along with governing failure modes and key parameters. In Table 3.1 **Error! Reference source not found.** the N_{sa} , N_b , N_{ba} is the steel, concrete breakout and bond strength of anchors respectively. For this study we are restricted to second method (breakout design method for cast-in anchors) with the focus on finding effective k factor value

Table3.1 Various Methods for Designing Rebars as Anchorages

| Method | End Anchorage | Cast-in Anchors Breakout | Adhesive/Grouted Anchors |
|------------------|----------------------------------|--|---|
| Design Standards | Chapter 25, ACI 318-19 | Chapter 17, ACI 318/ACI 349 | |
| Governing Eq. | Development length Eq. | Breakout Eq. | Uniform Bond stress Eq. |
| Strength | $N_{sa} = n \cdot A_s \cdot f_y$ | $N_b = k_c \cdot \lambda \cdot \sqrt{f'_c} \cdot h_{ef}^{1.5}$ | $N_{ba} = \lambda_a \cdot \tau_{cr} \cdot \pi \cdot d_b \cdot h_{ef}$ |
| Governs | N_{sa} | $\min (N_b, N_{sa})$ | $\min (N_{ba}, N_b, N_{sa})$ |
| Parameters | Development length | k_c factor | Bond stress |

The applicability of using provisions of adhesive anchors for normal deformed rebars (DRA/DWA) was experimentally tested and verified by (Chicchi et al., 2020). The uniform bond model presumes the group anchor strength as the function of the critical spacing of anchors, i.e., the bond strength will increase as the critical spacing between individual anchor increases. Theoretically, the uniform bond model imposes no limit on the strength of anchors with increasing embedment length. However, the group anchor strength is limited by concrete breakout failure mode, thus limiting the use of the bond model of ACI 318/ACI 349 for such connections.

3.2 Development Length Concept per ACI 318-19

The development length concept is established based on the constant bond stress (averaged) over the entire length of the embedded reinforcement. The rules and equations governing tension development length of deformed bars and deformed wires (DRAs and DWAs), according to Chapter 25 of ACI 318-19, are discussed in this section. The capacity of the connection is controlled by yielding of the deformed bars and deformed wires fully developed as per the Chapter 25 (ACI 318-19) provisions. The appropriate development length can be determined using

equations (Eq 14 and Eq 15) without considering confinement of reinforcement. According to Chapter 25 (25.4.2.3 and 25.4.2.4) of ACI 318-19, the development length (l_d) can be determined as:

$$l_d = \left(\frac{f_y \psi_t \psi_e}{25 \lambda \sqrt{f'_c}} \right) d_b \quad \text{Eq 14}$$

$$l_d = \left(\frac{3 f_y \psi_t \psi_e \psi_s}{40 \lambda \sqrt{f'_c} \frac{c_b + K_{tr}}{d_b}} \right) d_b \quad \text{Eq 15}$$

Here, ψ_t , ψ_e , and ψ_s are the bar location factor, bar coating factor, and sizing factor, respectively.

Whereas the factor λ is used for lightweight concrete, f_y is the yield stress of the bar, and f'_c is the concrete compressive strength. Eq. 14 is a simplified equation to calculate the development length of the bar, whereas Eq. 15 is more refined as it includes all effects controlling development length.

The factor $\frac{c_b + K_{tr}}{d_b}$ considers the effect of transverse reinforcement and concrete cover, is taken as

2.5. (if $K_{tr}=0$ for no transverse reinforcement).

4. EXPERIMENTAL STUDY

This chapter presents the experimental study on embed plates welded with straight DRAs and DWAs used as anchors.

4.1 Development of Test Matrix and Specimen Details

The test matrix and specimen details including bar type, size, layout and spacing was selected while considering the typical embedment plate design used in nuclear power plants. The thickness of reinforced concrete walls of nuclear related structures typically range from 2 ft to 5 ft. Hence, the bars (anchors) smaller than #11 bars are typically used in such structures to allow sufficient embedment length of anchors. In addition, multiple rebar anchors are (e.g., 2x2 3x3 4x4, 5x5 etc.) needed in general to provide appropriate tension capacity to embedment plates exceeding the design demand. Even with multiple rebar anchors, the tension capacity of embedment plates can be influenced by the rebar spacing. That is, the tension capacity can be controlled by the concrete breakout capacity if the anchors are too closely spaced resulting in reduction of concrete breakout surface. This effect is already catered in the design equations of ACI 349-13/ACI 318-19 as described in Chapter 2. The typical rebar anchorage space ranges from 3 in. to 9 in. in the application to safety related nuclear facilities. In this study, eight group anchor test specimens were designed considering design parameters associated with the embedment plates. The parameters included are bar size, bar type, layout, and bar spacing. These parameters are similar to what considered by Chicchi et al. (2020) (#6 bar with 4 in. spacing and 5x5 layout). However, different parameter values were selected to expand the database.

Table 4.1 presents details of the eight group anchor test specimens. As presented in the table, the focus was on the effects of (i) the bar layout (3x3 or 5x5), (ii) bar type (DRA or DWA), (iii) bar size ($d_b = 0.5$ in. dia., 0.625 in. dia.), and (iv) bar spacing ($s = 3$ in., 4.5 in., and 6 in.). All test specimens have straight bars that are embedded in concrete at their development length (l_d) per ACI 318-19. The material properties were measured by testing concrete cylinders and steel coupons in Bowen laboratory. For concrete, normal weight concrete ($f'_c = 6000$ psi) with $w/c = 0.36$, slump

= 4+-1 in., ½ in. aggregate was used. Detailed concrete mix design is provided in Appendix C. The concrete compressive strength was measured per ASTM C39 (ASTM, 2010) for each specimen on testing day. The coupon tests (standard uniaxial test) were conducted per ASTM E8 (ASTM, 2016) to measure yield and ultimate tensile strengths of the bars. The thickness of the embed plates is 1.5 in. for all specimens as presented in Table 4.1. Table 4.2 presents RC block dimensions of the eight group anchor test specimens. The RC block is post-tensioned to the laboratory floor to prevent uplift. As shown, all test specimens are 114 in. wide, 114 in. long, and 30 in. deep. These dimensions were determined so that post-tensioning forces (anchoring the RC block to the laboratory floor acting at 45° angles) would not interfere or overlap with the breakout cone (35° from the exterior anchor) of the concrete block specimen, as illustrated in Figure 4.2. In addition, the reinforcement mat was placed at the top and bottom of the blocks to avoid shear and flexural failures due to the large forces applied by the actuator at the midspan of the block. For tests # 1, 2, 5 and 6, #5 bars at 6 in. on center, and for tests # 3, 4, 7 and 8, #5 bars at 8 in. on center are used for the top and bottom mats in both directions. Figure 4.1 shows the cross-section details of the concrete block of 3x3 DWA 5/8 specimen. The detailed drawings for the eight group anchor test specimens are provided in Appendix B.

The expected failure mode using measured material properties of each test specimen is presented in Table 4.3. The yield strength (P_y) and tensile strength (P_u) of specimens were calculated by multiplying the measured yield stress (f_y) and ultimate tensile stress (f_u) with the area of the anchor bar (A_b) and number of anchors (n). They are compared with concrete breakout strength N_{cbg_keff} of each specimen to determine the governing failure mode. As presented, all test specimens are expected to fail in concrete breakout.

N_{cbg_keff} for a group anchor test specimen is calculated using the design equations in ACI 318-19 as presented in Eq (5). The modification factors $\psi_{ec,N}$, $\psi_{ed,N}$, $\psi_{c,N}$, and $\psi_{cp,N}$ denote eccentric loading, edge effects, uncracked concrete, and critical spacing of anchors to control splitting failure. A_{Nco} represents the projected surface area of a single anchor. A_{Nco} is the distance of 1.5 times the effective embedment depth (h_{ef}) on either side from the center of the anchor. A_{Nco} is obtained using Eq. (7). A_{Nc} represents the projected area of the group of anchors obtained by extending the failure

surface $1.5h_{ef}$ outward from the exterior row of anchors. N_b is the breakout strength of a single anchor in tension in cracked concrete. It is calculated using Eq (6).

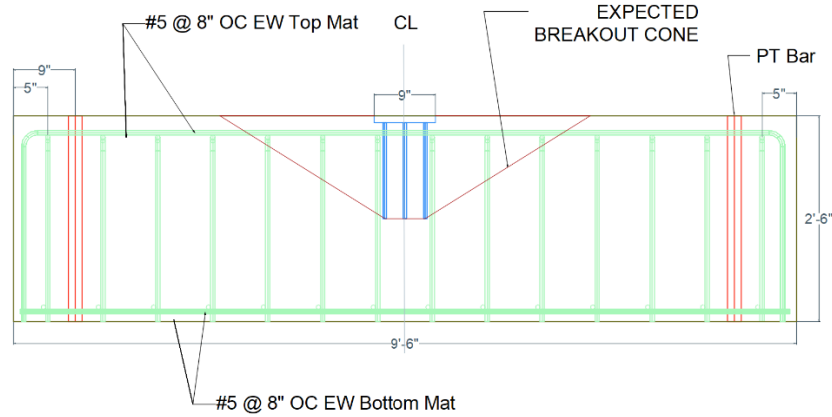


Figure 4.1 Cross-section of concrete block for 3x3 DWA 5/8 specimen

In Table 4.3 Expected failure modes of grouped anchor tests, the concrete breakout strength of each test specimen is computed using Eq. (5). However, k_c is replaced with k_{eff} values that are experimentally measured and back-calculated from previously conducted tests (Chicchi et al., 2020). The value of k_{eff} is 35.4 for the DRA specimens (tests # 1 and 2) and 31.4 for the DWA specimens (tests # 3, 4, 5, 6, 7, and 8). The design examples with detailed calculations are provided in Appendix A.

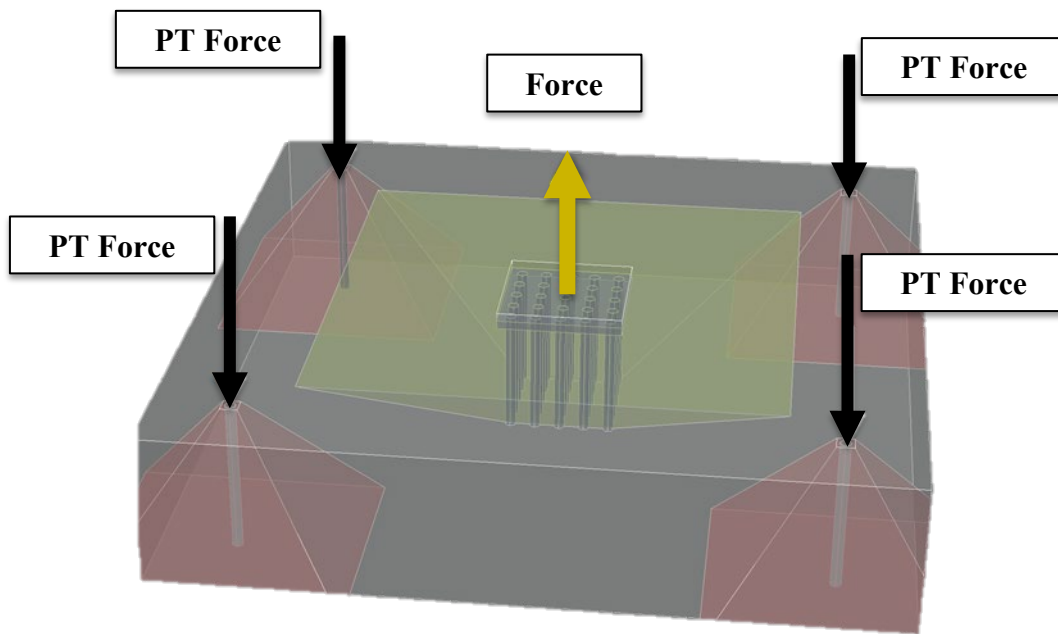


Figure 4.2 Concrete breakout cone with the effect of post-tensioning forces

Table 4.1 Test matrix of grouped anchor tests

| Test | Specimen | Type | Size | d_b (in.) | A_b (in ²) | n | s (in) | Bar Type | l_d (in) | l_{emb} (in) | f_y (ksi) | f_u (ksi) | t_p (in) | f'_c (psi) |
|------|------------|------|-------|----------------|-----------------------------|-----|-------------|-------------|---------------|-------------------|----------------|----------------|---------------|-----------------|
| 1 | 5x5-#5 | DRA | #5 | 0.625 | 0.31 | 25 | 3 | Straight | 11.6 | 11.75 | 69.37 | 95.72 | 1.5 | 7711 |
| 2 | 5x5-#5 | DRA | #5 | 0.625 | 0.31 | 25 | 3 | Straight | 11.6 | 11.75 | 69.37 | 95.72 | 1.5 | 7753 |
| 3 | 5x5-DWA4/8 | DWA | D-4/8 | 0.5 | 0.2 | 25 | 3 | Straight | 10.8 | 11.00 | 80.1 | 89.6 | 1.5 | 6521 |
| 4 | 5x5-DWA4/8 | DWA | D-4/8 | 0.5 | 0.2 | 25 | 3 | Straight | 10.8 | 11.00 | 80.1 | 89.6 | 1.5 | 5599 |
| 5 | 5x5-DWA5/8 | DWA | D-5/8 | 0.625 | 0.3067 | 25 | 3 | Straight | 13.6 | 14 | 82.1 | 88.7 | 1.5 | 7294 |
| 6 | 5x5-DWA5/8 | DWA | D-5/8 | 0.625 | 0.3067 | 25 | 3 | Straight | 13.6 | 14 | 82.1 | 88.7 | 1.5 | 6300 |
| 7 | 3x3-DWA5/8 | DWA | D-5/8 | 0.625 | 0.3067 | 9 | 4.5 | Straight | 13.6 | 14 | 82.1 | 88.7 | 1.5 | 6200 |
| 8 | 3x3-DWA5/8 | DWA | D-5/8 | 0.625 | 0.3067 | 9 | 6 | Straight | 13.6 | 14 | 82.1 | 88.7 | 1.5 | 6361 |

Table 4.2 Concrete block dimension of grouped anchor tests

| Test | Specimen | DRA/DWA | Size | h_{ef} (in) | Block Width (in.) | Block Length (in.) | Block Depth (in.) |
|------|------------|---------|-------|---------------|----------------------|-----------------------|----------------------|
| 1 | 5x5-#5 | DRA | #5 | 13.3 | 114 | 114 | 30 |
| 2 | 5x5-#5 | DRA | #5 | 13.3 | 114 | 114 | 30 |
| 3 | 5x5-DWA4/8 | DWA | D-4/8 | 12.5 | 114 | 114 | 30 |
| 4 | 5x5-DWA4/8 | DWA | D-4/8 | 12.5 | 114 | 114 | 30 |
| 5 | 5x5-DWA5/8 | DWA | D-5/8 | 15.5 | 114 | 114 | 30 |
| 6 | 5x5-DWA5/8 | DWA | D-5/8 | 15.5 | 114 | 114 | 30 |
| 7 | 3x3-DWA5/8 | DWA | D-5/8 | 15.5 | 114 | 114 | 30 |
| 8 | 3x3-DWA5/8 | DWA | D-5/8 | 15.5 | 114 | 114 | 30 |

Table 4.3 Expected failure modes of grouped anchor tests

| Test | Specimen | Size | n | s (in) | l_{emb} (in) | P_y (kips) | P_u (kips) | N_{cbg_keff} (kips) | k_{eff} | h_{ef} (in) | A_{nc} (in ²) | A_{nco} (in ²) | Failure Mode |
|------|------------|-------|-----|-------------|-------------------|-----------------|-----------------|---------------------------|-----------|------------------|--------------------------------|---------------------------------|--------------|
| 1 | 5x5-#5 DRA | #5 | 25 | 3 | 11.75 | 537.6 | 741.8 | 254.1 | 35.4 | 13.3 | 2678 | 1580 | Breakout |
| 2 | 5x5-#5 DRA | #5 | 25 | 3 | 11.75 | 537.6 | 741.8 | 254.8 | 35.4 | 13.3 | 2678 | 1580 | Breakout |
| 3 | 5x5-DWA4/8 | D-4/8 | 25 | 3 | 11.00 | 400.5 | 448.0 | 195.3 | 31.4 | 12.5 | 2450 | 1406 | Breakout |
| 4 | 5x5-DWA4/8 | D-4/8 | 25 | 3 | 11.00 | 400.5 | 448.0 | 180.9 | 31.4 | 12.5 | 2450 | 1406 | Breakout |
| 5 | 5x5-DWA5/8 | D-5/8 | 25 | 3 | 13.75 | 629.5 | 680.1 | 259.0 | 31.4 | 15.5 | 3422 | 2162 | Breakout |
| 6 | 5x5-DWA5/8 | D-5/8 | 25 | 3 | 13.75 | 629.5 | 680.1 | 240.7 | 31.4 | 15.5 | 3422 | 2162 | Breakout |
| 7 | 3x3-DWA5/8 | D-5/8 | 9 | 4.5 | 13.75 | 226.6 | 244.8 | 214.9 | 31.4 | 15.5 | 3080 | 2162 | Breakout |
| 8 | 3x3-DWA5/8 | D-5/8 | 9 | 6 | 13.75 | 226.6 | 244.8 | 241.9 | 31.4 | 15.5 | 3422 | 2162 | Breakout |

4.2 Test Setup and Loading Protocol

The tension loading was applied to the steel plates at the top of the specimen using a 660 kip actuator, while the specimen is post-tensioned to the floor as shown in Figure 4.3. The actuator is also connected to the cross beam of the loading frame. The loading frame has already been built and used at Bowen Laboratory. This loading frame has been designed (and used in the past) to conduct tests with maximum applied loading up to 660 kips, which is the limit of the actuator capacity used to conduct the tests. The applied loading was increased monotonically until the failure of the specimen occurred in terms of loss of load carrying capacity due to concrete breakout failure or rupturing of the steel bars. Additionally, small loading-unloading cycles with load levels up to 20 kips or 10% of the expected failure strength were performed at the beginning of the test to check the loading system, sensor behavior, or elastic behavior of the specimen.

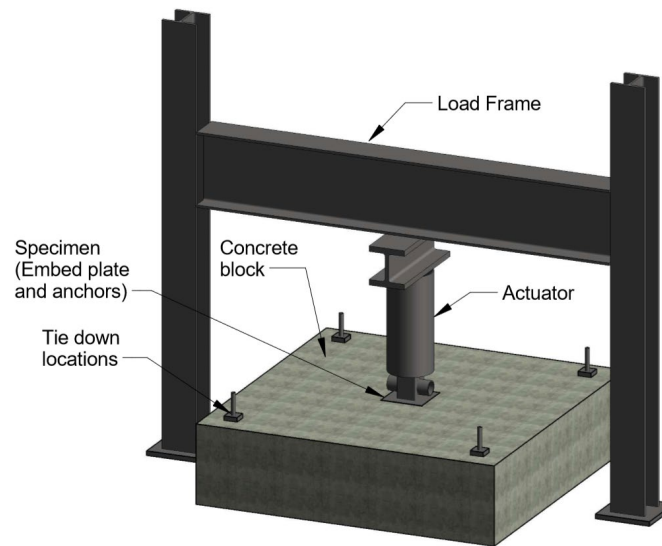


Figure 4.3 Test frame with the test specimen (Chicchi et al., 2020)

4.3 Sensor Layout

The behavior of the group anchor test specimens is measured using displacement transducers (DTs) and strain gages (SGs). The vertical displacement of group anchor specimens within the concrete cone is measured using linear variable displacement transducers (LVDTs, DT3 ~ DT6) as shown

in Figure 4.5. The LVDTs are placed on the concrete surface in a circular pattern at 1.5 times h_{ef} from the embed plate, as shown in Figure 4.4(a). The vertical displacement of the embed plate was measured using two displacement transducers (1 and 2). Two additional LVDTs are placed on the laboratory floor along adjacent sides of the RC block to determine the potential uplift of the specimen. The axial strains of the anchors are measured by installing strain gages (SGs) along the longitudinal axis of the bar. The strain gages on anchors are installed at a distance of 1 inch (2.5 cm) below the embed plate. Figure 4.4 (b), (c), and (d) illustrate SG configuration for specimens 1 through 8.

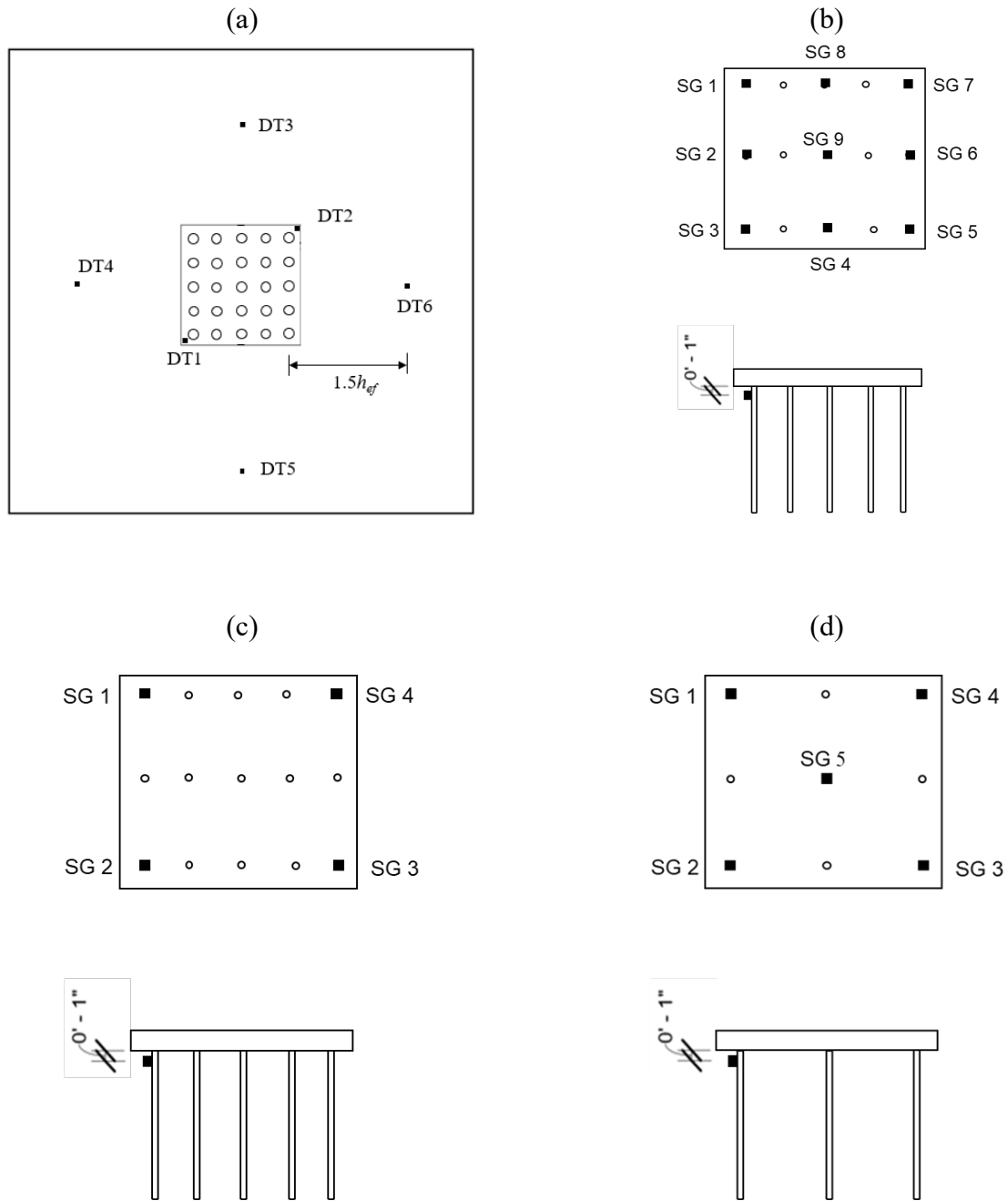


Figure 4.4 Sensor layout for grouped anchor specimens: (a) displacement transducers, (b) strain gages for test no 1,2,3 and 4 (c) strain gages for test 5 and 6 and (d) strain gages for test 7 and 8

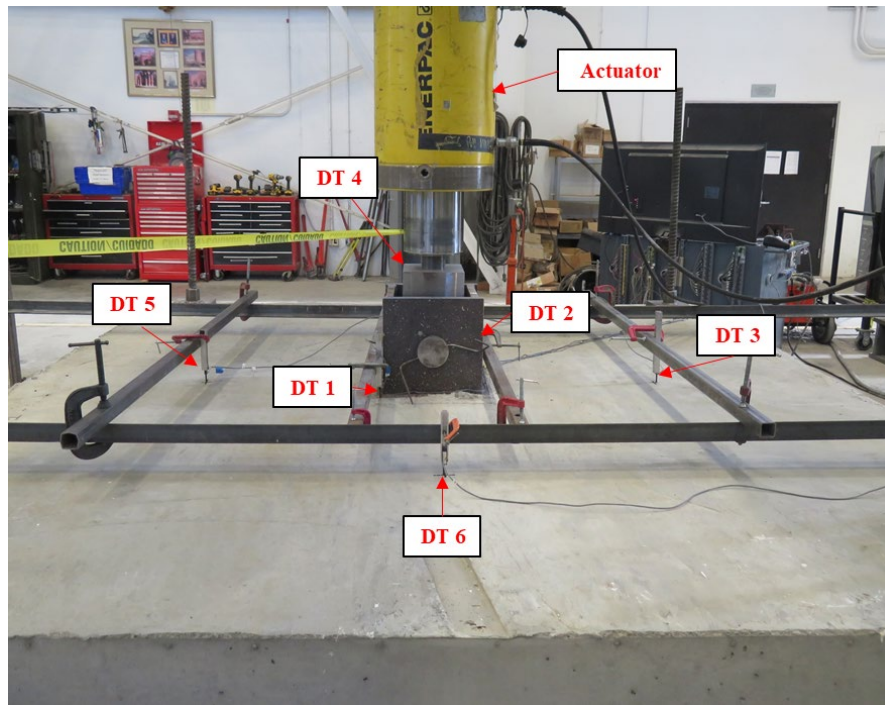


Figure 4.5 Linear variable displacement transducers (LVDTs, DT3 ~ DT6) installed on the concrete surface of the specimen

5. TEST RESULTS

The results of group anchor tests are summarized in **Error! Reference source not found.** Table 5.1. Results and details of each test are described in subsequent sections

Table 5.1 Summary of Test Results

| Specimen | Layout | n | s (in) | h_{ef} (in) | f_c' (psi) | P_y (kips) | P_u (kips) | N_{cbg_keff} (kips) | P_{max} (kips) | Failure Mode | Back calculate k_{eff} | Breakout Angle (degrees) |
|----------|------------|-----|----------|---------------|--------------|--------------|--------------|------------------------|------------------|---------------------|--------------------------|--------------------------|
| 1 | 5x5-DRA #5 | 25 | 3 | 13.3 | 7771 | 537.6 | 741.8 | 254.1 | 243.2 | Breakout | 33.88 | 34.22 |
| 2 | 5x5-DRA #5 | 25 | 3 | 13.3 | 7753 | 537.6 | 741.8 | 254.8 | 234.9 | Breakout | 32.63 | 36.77 |
| 3 | 5x5-DWA4/8 | 25 | 3 | 12.5 | 6251 | 400.5 | 448.0 | 195.3 | 225.1 | Breakout | 36.20 | 36.23 |
| 4 | 5x5-DWA4/8 | 25 | 3 | 12.5 | 5599 | 400.5 | 448.0 | 180.9 | 207.5 | Breakout | 36.01 | 30.15 |
| 5 | 5x5-DWA5/8 | 25 | 3 | 15.5 | 7294 | 629.5 | 680.1 | 259 | 283.15 | Breakout | 34.33 | 26.25 |
| 6 | 5x5-DWA5/8 | 25 | 3 | 15.5 | 6300 | 629.5 | 680.1 | 240.7 | 295.2 | Breakout | 38.51 | 26.56 |
| 7 | 3x3-DWA5/8 | 9 | 4.5 | 15.5 | 6200 | 226.6 | 244.8 | 215.8 | 210.4 | Pullout | - | - |
| 8 | 3x3-DWA5/8 | 9 | 6 | 15.5 | 6361 | 226.6 | 244.8 | 241.9 | 235 | Rupture/ Pullout | - | - |

5.1 Test # 1 - 5x5 DRA # 5

Test 1 was conducted on the 5x5 DRA #5 specimen with effective embedment length (h_{ef}) of 13.3 in. The predicted breakout strength of 254.1 kips was calculated using measured concrete strength, and k_{eff} of 35.4 used for DRAs. The specimen experienced a breakout failure at 243.2 kips (P_{max}), 4.3% (11.6 kips) less than the predicted breakout strength (N_{cbg}) of 254.1 kips. The average vertical displacement of the embed plate measured using LVDTs (DT1, DT2) at P_{max} is approximately 0.0325 in. Figure 5.1 shows the applied load-displacement (P- Δ) response of the tested specimen. The failure load corresponds to a back-calculated effective k (k_{eff}) value of 33.88, only 4.3% less than the estimated value of 35.4. The breakout failure load (P_{max} =243.2 kips) is well below the measured anchor yield strength (537.6 kips). Clearly, the concrete breakout is the governing failure mode for this specimen.

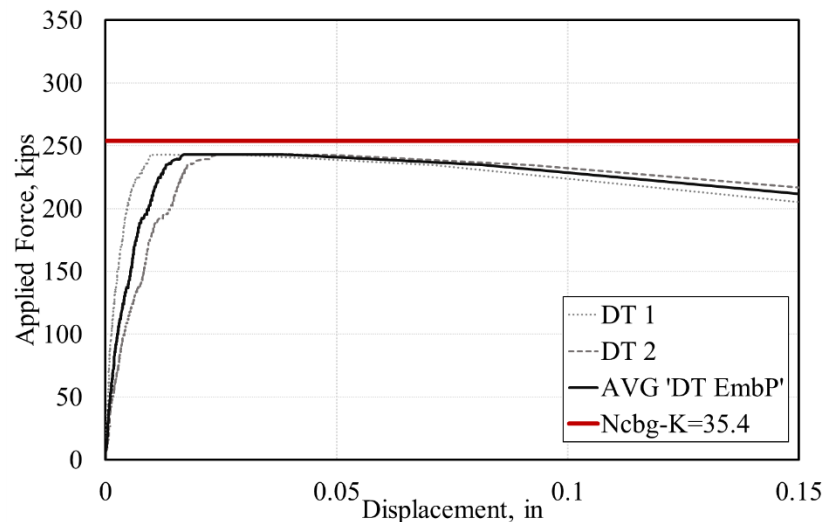


Figure 5.1 Applied force-displacement (P- Δ) response of Test 1

Figure 5.2 shows the cracks on the surface of the concrete after breakout failure. The cracks are formed in a circular ring pattern on the surface of the specimen. The distances are measured from the exterior anchor to the crack, depicting the boundaries of breakout cone on the surface. The

measured crack distance from exterior anchors varies from 12 in. to 23 in. with an average distance of $1.1h_{ef}$. No cracks were observed until the load reached P_{max} .

The breakout cone was removed from the specimen to observe the failure plane and breakout cone, as shown in Figure 5.3(a) and (b). The breakout cone angle measured from the horizontal varies from 31.25 degrees to 37.56 degrees with an average breakout cone angle of 34.22 degrees. The angle of concrete cone conforms to the ACI prescribed angle of 35 degrees (CCD method).

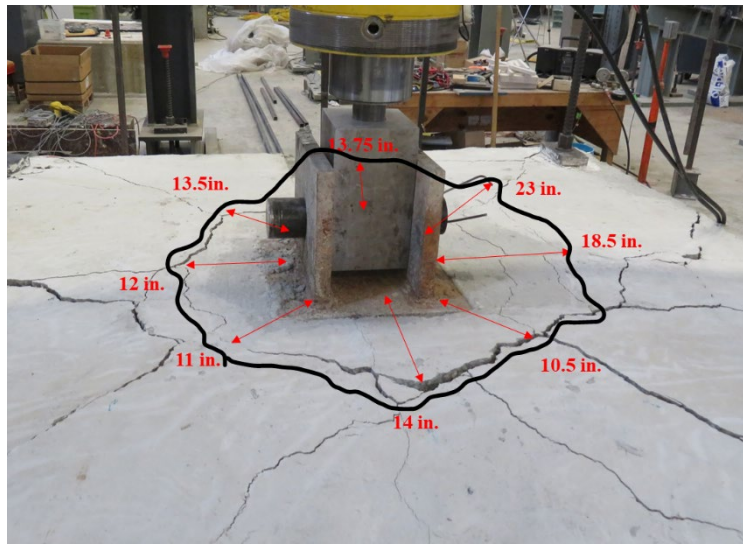


Figure 5.2 Plan view of cracks formed on the concrete surface

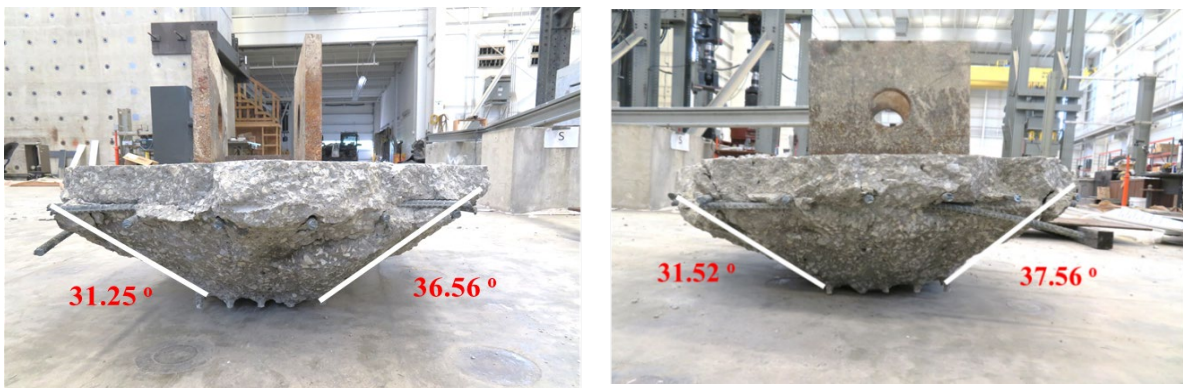


Figure 5.3 Breakout cone with an average angle of 34.22 degrees

5.2 Test # 2 - 5x5 DRA # 5

Test 2 was conducted on the 5x5 DRA #5 specimen with effective embedment length (h_{ef}) of 13.3 in., same as of test 1. This DRA specimen also failed in concrete breakout similar to the previous test specimen. The test specimen failed at 234.9 kips (P_{max}), which is 7.8% (19.9 kips) less than the N_{cbg} (254.8 kips). The average vertical displacement measured by LVDTs (DT 1 and DT2) is 0.028 in. at failure. The back-calculated effective k value of 32.5 is less than the predicted k_{eff} of 35.4. Figure 5.4 shows the applied load-displacement (P- Δ) response of the test specimen.

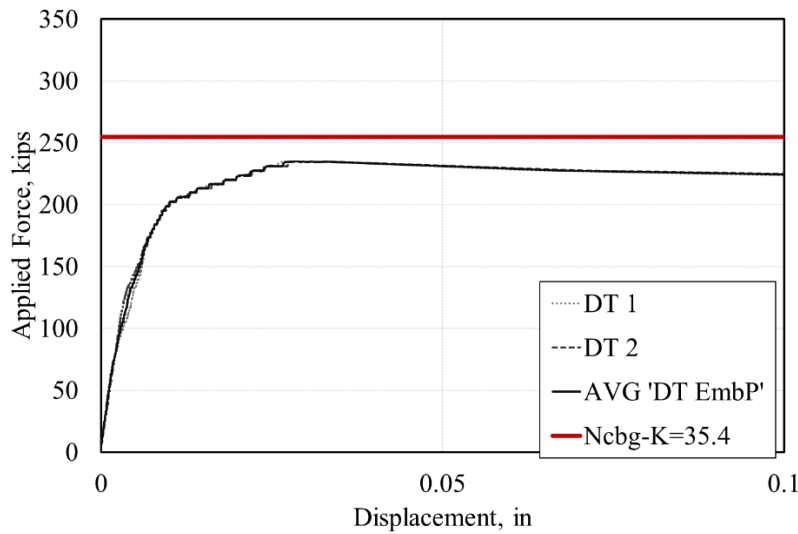


Figure 5.4 Applied force-displacement (P- Δ) response of Test 2

Figure 5.5 illustrates the formation of cracks on the concrete surface due to tension loading. The cracks encircle the embed plate, as shown in Figure 5.5. The average distance from exterior anchors is 19.95 in. ($1.06 h_{ef}$), which is less than the code specified value of $1.5 h_{ef}$.

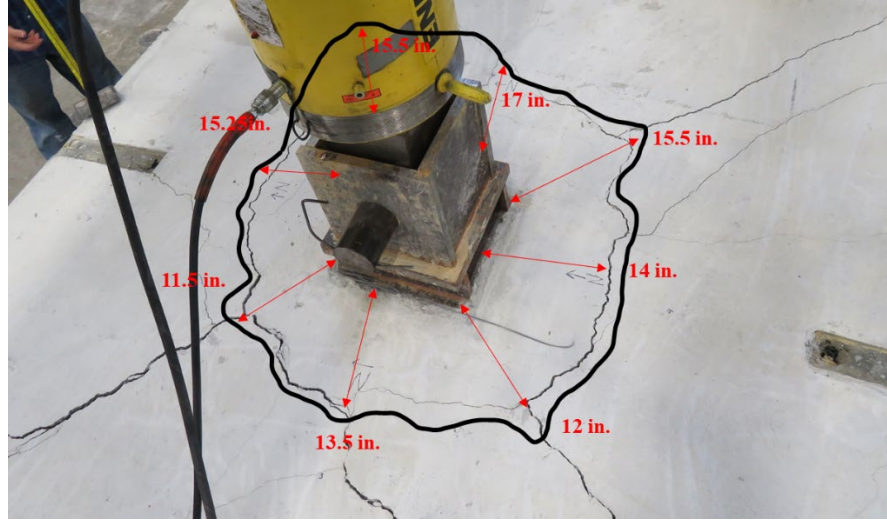


Figure 5.5 Plan view of cracks and formed on the concrete surface

The breakout cone was taken out from the concrete block. The breakout cone is shown in Figure 5.6 (a) and (b). The observed breakout cone angle varies from 35.40 degrees to 38.86 degrees with an average breakout cone angle of 36.77 degrees, which is close to the code specified cone angle of 35 degrees.



Figure 5.6 Breakout cone with an average angle of 36.77 degrees

5.3 Test # 3 – 5x5 DWA 4/8

Test 3 was conducted on the specimen 5x5 DWA 4/8 with an effective embedment length of 12.5 in. The predicted breakout strength (N_{cbg} =195.3 kips) was calculated using measured properties, and k_{eff} of 31.4 (DWA). Figure 5.7 shows the applied load-displacement (P- Δ) response of the

tested specimen. The test specimen failed in concrete breakout at 225.1 kips (P_{max}), which is 15.2% (29.2 kips) greater than the predicted N_{cbg} (195.3 kips). The vertical displacement measured at maximum load is approximately 0.047 in. The effective k value of 36.2 back-calculated using the failure load (P_{max}) is somewhat higher than the k_{eff} (31.4), used for initial calculations. The steel strength (P_y , P_u) of the connection was calculated using measured yield stress and tensile stress of the anchors. The breakout failure load (P_{max} =235 kips) is well below the yield strength (P_y =400.5 kips) and tensile strength (P_u =448 kips) of the anchor. Clearly, the concrete breakout is the governing failure mode for this specimen.

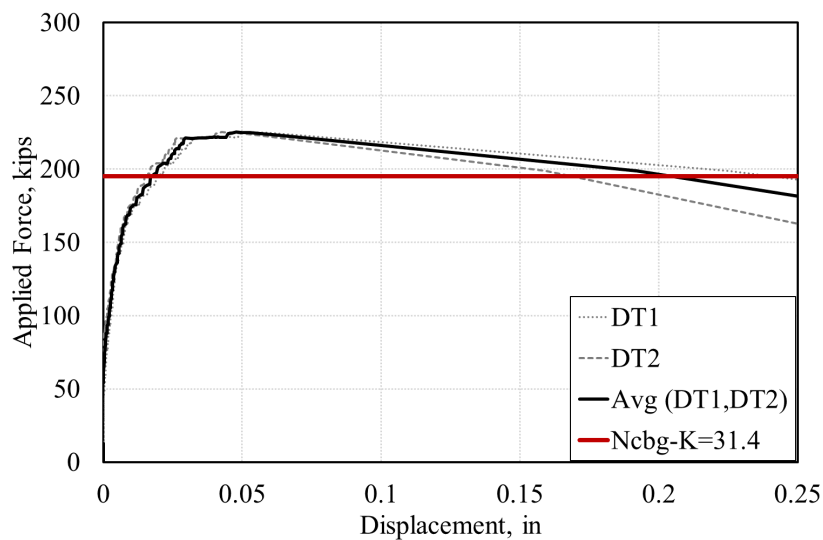


Figure 5.7 Applied force-displacement (P-Δ) response of test 3

Figure 5.8 shows the cracks after failure, formed in a circular ring pattern on the surface of the specimen. The distances are measured from the exterior anchor to the crack, depicting the boundaries of breakout cone. The measured crack distance from exterior anchors varies from 12.5 in. to 18 in. ($1h_{ef}$ - $1.44h_{ef}$) with an average distance of $1.21h_{ef}$. The measured distance from the result is little less than the code prescribed distance of $1.5h_{ef}$. No cracks were observed until the load reaches P_{max} .

The breakout cone was removed from the specimen to observe the failure plane and breakout cone, as shown in Figure 5.9 (a) and (b). The breakout cone angle in horizontal direction varies from 33

degrees to 41.05 degrees with an average breakout cone angle of 36.23 degrees. The angle of the concrete cone conforms to the ACI prescribed angle of 35 degrees (CCD method).

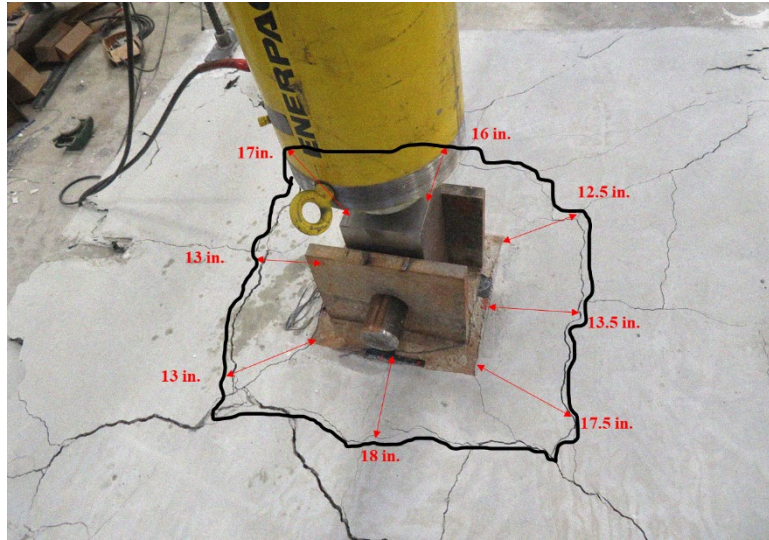


Figure 5.8 Plan view of cracks formed on the concrete surface

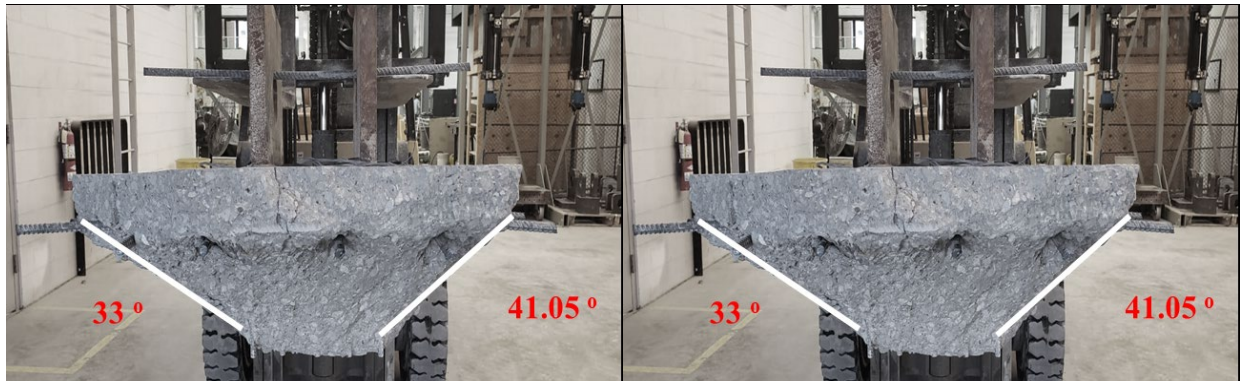


Figure 5.9 Breakout cone with average angle of 36.23 degrees

5.4 Test # 4 – 5x5 DWA 4/8

Test 4 was conducted on the similar 5x5 DWA 4/8 specimen as of test 3. This specimen also fails in the concrete breakout at 207.5 kips (P_{max}). Figure 5.10 shows the applied load-displacement (P- Δ) response of the tested specimen. The maximum load of 207.5 Kips (P_{max}) is 14.7% (26.6 kips)

higher than the N_{cbg} (180.9 kips). The vertical displacement measured at P_{max} is approximately 0.048 in. The back-calculated k_{eff} value of 36.02 is somewhat higher than the k_{eff} (31.4), but similar to effective k observed in previous test (36.2).

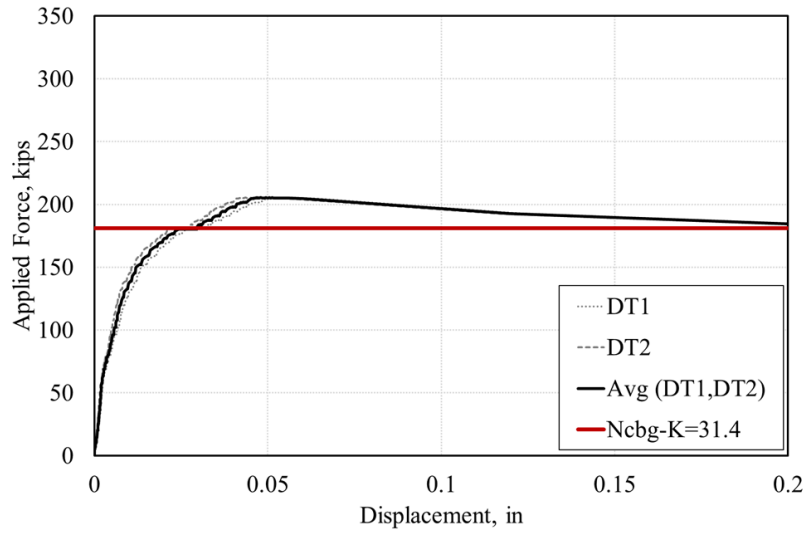


Figure 5.10 Applied force-displacement (P-Δ) response of test 4

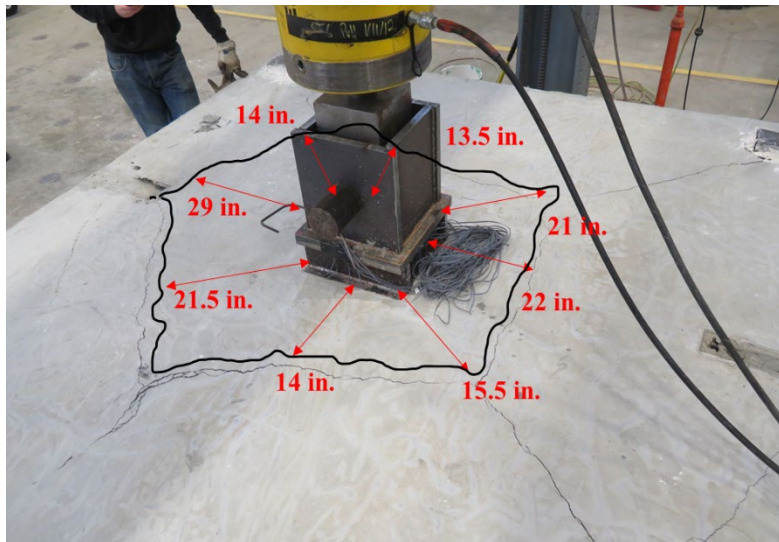


Figure 5.11 Plan view of cracks formed on concrete surface

The breakout cone was removed from specimen to observe the breakout cone angle as shown in Figure 5.12 (a) and (b). The breakout cone angle varies from 32.61 degrees to 31.57 degrees with an average breakout cone angle of 30.15 degrees, which is less than the previous test 3 (36.23).

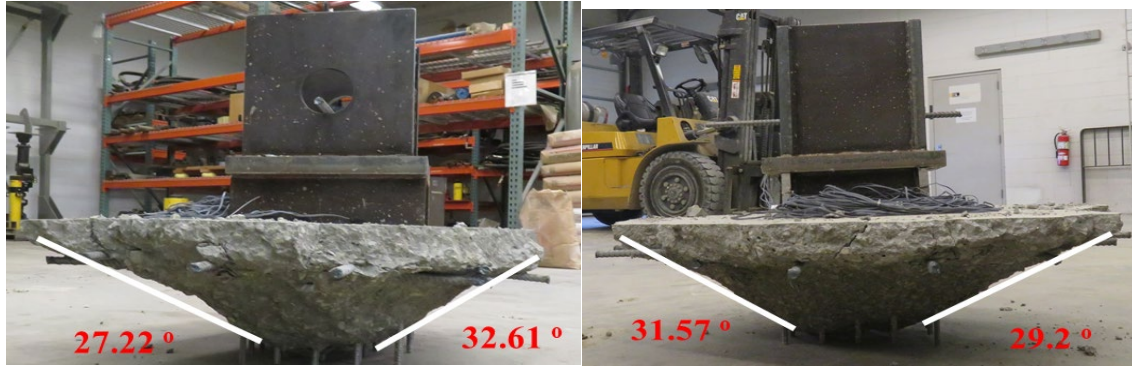


Figure 5.12 Breakout cone with average angle of 30.15 degrees

5.5 Test # 5 – 5x5 DWA 5/8

Test 5 consists of a 5x5 DWA 5/8 specimen with an embedment length of 15.5 in. The predicted breakout strength of 259 kips was calculated using measured concrete strength, and k_{eff} of 31.4 used for DWAs. Figure 5.13 shows the applied load-displacement ($P-\Delta$) response of the test specimen. The test results in breakout failure at 283.15 kips, 9.32% greater than the predicted breakout strength ($N_{cbg} = 259$ kips). The average vertical displacement measured using LVDTs (DT1, DT2) at P_{max} is approximately 0.066 in. The failure load corresponds to a back-calculated k_{eff} value of 34.33. The breakout failure load ($P_{max}=283.15$ kips) is well below the anchor yield strength (629.5 kips).

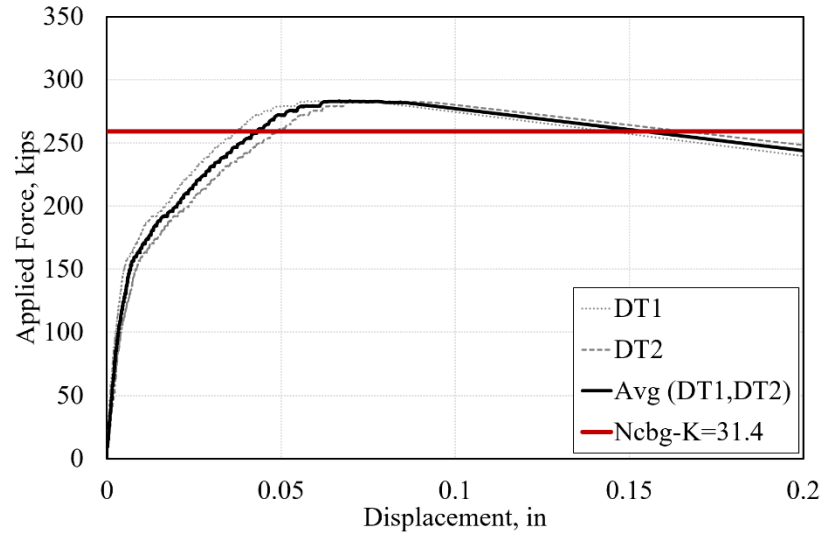


Figure 5.13 Applied force-displacement (P-Δ) response of test 5

Figure 5.14 shows the crack pattern formed on the concrete surface. The cracks from exterior anchors occurred at 31.75 in.(average), equivalent to 2 h_{ef} . This corresponds to a wider breakout cone as compared to predicted distance of 1.5 h_{ef} given by the code.

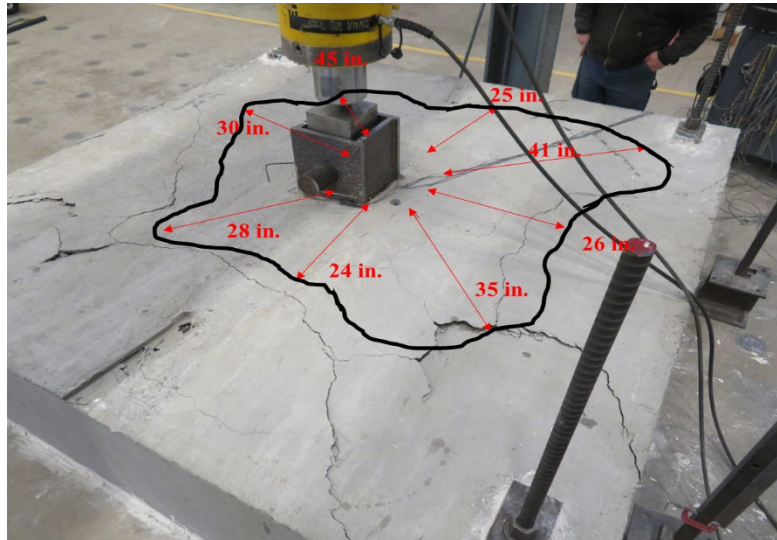


Figure 5.14 Plan view of cracks and formed on the concrete surface

The breakout cone was observed by carefully removing concrete cone from the specimen. The breakout cone is shown in Figure 5.15 (a) and (b). The breakout cone angle varies from 30.3

degrees to 20.5 degrees with an average breakout cone angle of 26.25 degrees, which is less than the previous tests 3 and 4 (36.23 degrees, 30.15 degrees)



Figure 5.15 Breakout cone with average angle of 26.25 degrees

5.6 Test # 6 – 5x5 DWA 5/8

Test 6 was conducted on the 5x5 DWA 5/8 specimen, same as of test 5. The failure mode and breakout strengths are summarized in Table 5.1. This DWA 5/8 specimen also failed in a breakout similar to previous DWA specimens. The test specimen failed in the concrete breakout at 295.2 kips (P_{max}), which is 22.6% (54.5 kips) greater than the N_{cbg} (240.7 kips). The back-calculated effective k value of 38.5 is higher than the predicted k_{eff} of 31.4. The vertical displacement measured at P_{max} is approximately 0.075 in. Figure 5.16 shows the applied load-displacement (P - Δ) response of the test specimen

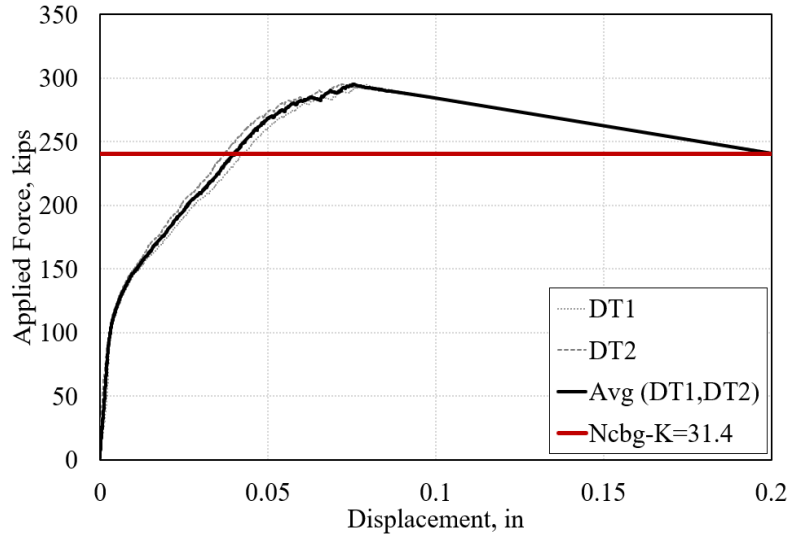


Figure 5.16 Applied force-displacement (P-Δ) response of test 6

Figure 5.17 shows the crack pattern formed on the concrete surface. The measured crack distance from the exterior anchor varies from 21 in. to 38 in. ($1.35h_{ef}$ - $2.4h_{ef}$) with an average distance of $1.9h_{ef}$, somewhat higher than the code prescribed value of $1.5h_{ef}$. The concrete cone was removed from the specimen as shown in Figure 5.18. The average breakout cone angle is 26.56 degrees, which is close to the test # 5 cone angle of 26.25 degrees.

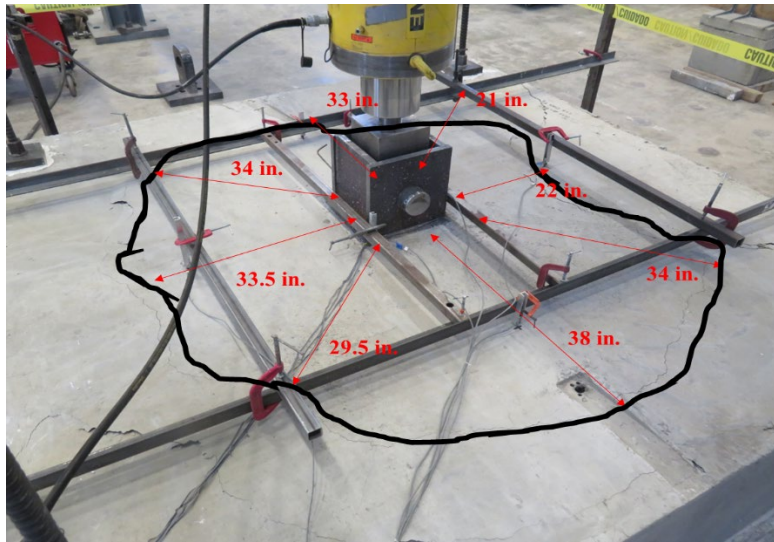


Figure 5.17 Plan view of cracks and formed on the concrete surface



Figure 5.18 Breakout cone with an average angle of 26.56 degrees

5.7 Test # 7 – 3x3 DWA 5/8

Test # 7 was designed to observe the effect of spacing on anchorage capacity. It was configured to have 3x3 DWA 5/8 with 4.5 in. spacing. The calculated breakout strength was 215.8 kips, and the tensile strength of anchors was 244.8 kips. The breakout failure was the anticipated failure mode for this specimen. However, the specimen failed in pullout at a maximum tensile load of 210.4 kips before reaching to breakout or tensile strength, as shown in Figure 5.20 (a) and (b). Figure 5.19 shows the load-displacement response of the tested specimen.

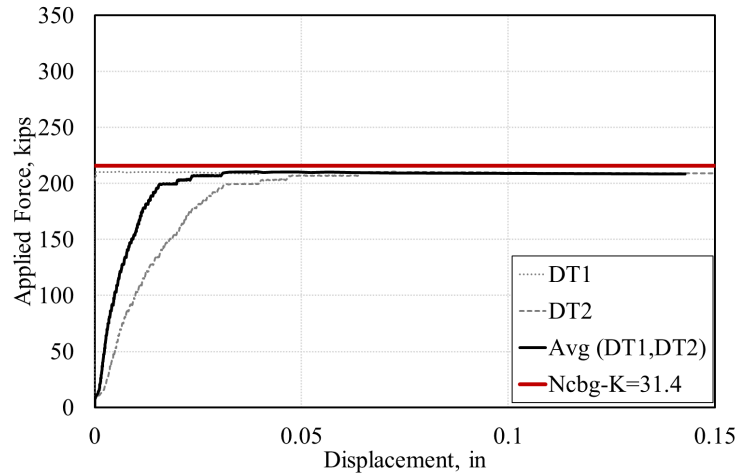


Figure 5.19 Applied force-displacement (P-Δ) response of test



Figure 5.20 (a) and (b) Illustrates Pull-out failure

5.8 Test # 8 – 3x3 DWA 5/8

Test # 8 was also designed to observe the effect of spacing on breakout strength by having 3x3 DWA 5/8 with 6 in. anchor spacing. The test experienced a complex failure phenomenon, which is a mixture of pullout and rebar rupture. The calculated breakout strength of 241.9 kips and anchor tensile strength of 244.8 kips were very close. At maximum failure load of 235 kips, four out of nine bars, ruptured as shown in Figure 5.22. On further load application, three more bars ruptured

and two bars pulled out of the specimen as shown in Figure 5.23 and Figure 5.24 respectively. Hence, the specimen failed in both rebar rupture and pullout, but rebar rupture is the predominant failure mode. Due to low bond strength of DWAs, the pullout failure was always a relevant failure mode. Figure 5.23 clearly indicates that DWA bars have adequate weld capacity, as none of the bars experienced weld failure. Figure 5.21 shows the applied load-displacement ($P-\Delta$) response of the test specimen.

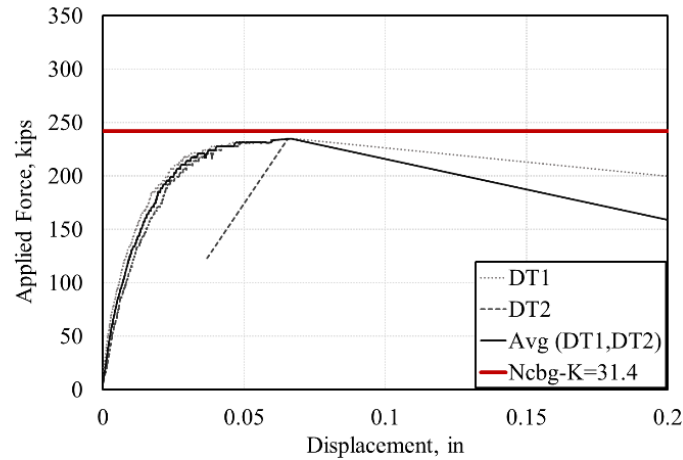


Figure 5.21 Applied force-displacement ($P-\Delta$) response of test 8



Figure 5.22 Pulled out and Ruptured bars



Figure 5.23 Ruptured bars



Figure 5.24 Pulled out bars

5.9 Summary of Test Results

Table 5.1 summarizes the test results, including specimen type, measured concrete strengths, measured yield strength (P_y), measured tensile strength (P_u), calculated breakout strength (N_{cbg} using k_{eff} of 31.4 and 35.4), and failure load (P_{max}). It also indicates governing failure mode, effective k (k_{eff}), and breakout cone angles for all tested specimens. The experimentally observed breakout strengths are less than the yield strengths (P_y) and tensile strength (P_u) of the anchors up to 50-60 %. Hence, strength calculations based on steel yielding and rupture are unconservative as they overestimate the connection capacity. Therefore, breakout checks are recommended for connections designed in this manner. The observed breakout strengths are close to the predicted breakout strengths of the specimens calculated using code equations and the effective k (k_{eff}) reported by (Chicchi et al., 2020). The average effective k measured in this study is 36.26 for DWA specimens, which is 11% higher than k_{eff} of 31.4 (Chicchi et al., 2020). Whereas, the average effective k measured in this study for DRA specimens was 33.25, which is 6.5% less than k_{eff} of 35.4 based on the research by (Chicchi et al., 2020). The failure plane varies from 26 to 36 degrees, whereas code prescribed value is 35 degrees. The average breakout angle is 35.5 degrees for DRAs and 29.8 degrees for DWAs. Test #7 (3x3 DWA5/8, 4.5in. spacing) failed in pullout, and test #8 (3x3 DWA5/8, 6in. spacing) failed in pullout and rebar rupture, respectively. Hence, the effects of anchor spacing on breakout strengths could not be determined. These tests failed in pullout and rebar rupture before reaching their anticipated breakout capacities.

6. CONCLUSIONS AND FUTURE WORK

The test results unconditionally show the significance of breakout strengths in connections designed in this manner. Concrete breakout capacities overrule the full development length concept in ACI 349 code, which considers only yield or rupture failure for bars. The tensile capacity of such connections (steel plate with welded DRAs/DWAs) based on yield or rupture strengths results may lead to a significant overestimation of embedment capacity. Thus, the tension strength of the embed plate welded with DRAs and DWAs used in safety-related nuclear facilities may be limited by concrete breakout failure. However, other failure modes, pullout and, rupture should also be examined before finalizing the strength of these connections. The average back-calculated effective k value of 33.25 for DRAs and 36.26 for DWAs matches closely with the $k_c=35$ value of post-installed anchors.

The scope of the testing program was limited to specific bar sizes (5/8", 4/8" dia), spacing (6 in.), and design concrete compressive strength (6000 psi). The spacing effect on concrete breakout capacities of such connections could not be observed as the last two specimens failed in pullout and rebar rupture, respectively. Hence additional testing is required with different bar sizes, anchors spacing, and concrete strengths with various configurations (e.g., 2x2, 3x3, 4x4, etc.) to authenticate the design value of effective k used for estimating breakout strengths of such assemblies. Single anchor test specimens are under study to analyze the bond behavior and applicability of the bonded anchor models to such connections. There is a dire need to carry out analytical and parametric studies based on experimental results.

REFERENCES

- ACI Committee 355. (2019a). 355.2-19: Qualification of Post-Installed Mechanical Anchors in Concrete (ACI 355.2) and Commentary. American Concrete Institute 38800 Country Club Drive Farmington Hills, MI 48331.
- ACI Committee 355. (2019b). 355.4-19: Qualification of Post-Installed Adhesive Anchors in Concrete and Commentary. American Concrete Institute 38800 Country Club Drive Farmington Hills, MI 48331.
https://www.concrete.org/store/productdetail.aspx?ItemID=355419&Format=DOWNLOAD&Language=English&Units=US_Units
- ASTM. (2010). Standard test method for compressive strength of cylindrical concrete specimens. ASTM C39. ASTM International, West Conshohocken, PA, 2010.
- ASTM. (2016). ASTM E8 / E8M-16a, Standard Test Methods for Tension Testing of Metallic Materials. ASTM E8, ASTM International, West Conshohocken, PA, 2016.
https://doi.org/10.1520/E0008_E0008M-16A
- Bazant, Z. P., & Asce, F. (n.d.). SIZE EFFECT IN BLUNT FRACTURE: CONCRETE, ROCK, METAL.
- Chicchi, R., Seo, J., Varma, A. H., Bradt, T., Lafayette, W., Lafayette, W., Lafayette, W., & Lafayette, W. (2017). Consideration of Breakout Failure Modes in Design of Attachments To Concrete Structures.
- Chicchi, R., Varma, A. H., Seo, J., Bradt, T., & Zhang, K. (2020). EXPERIMENTAL TESTING OF TENSION-LOADED DEFORMED ANCHORS IN CONCRETE. *ACI Structural Journal*.
- Eligehausen, R. (2006). Anchorage in concrete construction (R. Mallee & J. F. Silva (eds.)) [Book]. Ernst & Sohn.
- Eligehausen, R., & Ozbolt, J. (n.d.). 876 INFLUENCE OF CRACK WIDTH ON THE CONCRETE CONE FAILURE LOAD.
- Eligehausen, R., & Sawade, G. (1989). A fracture mechanics based description of the pullout behavior of headed studs embedded in concrete. *Fracture Mechanics of Concrete Structures*, 281–299. <https://doi.org/10.18419/opus-7930>
- Eligehausen, R., & Tamas Balogh. (1995). Behaviour of Fasteners Loaded in Tension in Cracked Concrete. *ACI Structural Journal*, 92(3), 365–379.

- Fuchs, W., Eligehausen, R., & Breen, J. E. (1995). Concrete capacity design (CCD) approach for fastening to concrete. *ACI Structural Journal*, 92(1), 73–94. <https://doi.org/10.14359/1533>
- Mahrenholtz, C., Eligehausen, R., & Reinhardt, H. W. (2015). Design of post-installed reinforcing bars as end anchorage or as bonded anchor. *Engineering Structures*, 100(June 2013), 645–655. <https://doi.org/10.1016/j.engstruct.2015.06.028>
- Mahrenholtz, C., Eligehausen, R., & Reinhardt, H. W. (2020). Qualification and design of cast-in-place and post-installed reinforcing bar anchorages. *ACI Structural Journal*, 117(2), 3–16. <https://doi.org/10.14359/51720192>
- Mahrenholtz, P., & Eligehausen, R. (2015). Post-installed concrete anchors in nuclear power plants: Performance and qualification. *Nuclear Engineering and Design*, 287, 48–56. <https://doi.org/10.1016/j.nucengdes.2015.03.004>
- Nilforoush, R. (2017). Anchorage in Concrete Structures: Numerical and Experimental Evaluations of Load-Carrying Capacity of Cast-in-Place Headed Anchors and Post-Installed Adhesive Anchors (Doctoral dissertation, Luleå University of Technology).

APPENDIX A

Design Example 1

Design Calculations

Test # 3 5x5DWA $\frac{4}{8}$ ■

1. Data

$f'_c := 6000\text{psi}$ compressive strength of the concrete, psi

Steel Anchors Properties

| | |
|-------------------------|--------------------------------|
| Type | DWA |
| $F_y := 70\text{ksi}$ | Nominal Yield strength of bar |
| $d_b := 0.5\text{in}$ | Dia of #5 DWA bar |
| $A_s := 0.2\text{in}^2$ | Area of #5 DWA bar |
| $n := 25$ | Number of Anchors |
| $s := 3\text{in}$ | Spacing between anchors (bars) |

Steel Embedment Plate

| | |
|---------------------|------------------------------------|
| $B := 15\text{in}$ | Embed plate dimensions 15in x 15in |
| $L := 15\text{in}$ | |
| $t := 1.5\text{in}$ | Embed plate thickness |

2. Developement Length, l_d

| | |
|-----------------|---|
| $\lambda := 1$ | For normal weight concrete |
| $\psi_t := 1$ | rebar location factor |
| $\psi_e := 1$ | rebar coating factor |
| $\psi_s := 0.8$ | rebar size factor (0.8 for bars less than #6) |

$$C_{ktr} := 2.5$$

$$\frac{c + k_{tr}}{d_b} = 2.5 \quad \text{ACI 318-14 Section 25.4.2.3}$$

$$l_d := \left[\frac{3 \cdot F_y \cdot \psi_t \cdot \psi_e \cdot \psi_s}{40 \cdot \lambda \cdot (\sqrt{f'_c \cdot \text{psi}}) \cdot C_{ktr}} \right] \cdot d_b$$

Development length for deformed bars or deformed wires per ACI 318-14 Section 25.4.2.3

$$l_d = 10.84 \text{ in}$$

$$h_f := l_d + t = 12.34 \text{ in}$$

Effective Anchor length including steel plate

$$h_{ef} := 12.5 \text{ in}$$

Rounding off to next 0.5

3. Nominal Steel Strength of Anchors in Tension, N_s (ACI 318-19 Section 17.6.1.2)

$$N_{sa} := A_s \cdot F_y = 14 \cdot \text{kip}$$

Nominal yeild strength of a single anchor

$$N_s := n \cdot A_s \cdot F_y = 350 \cdot \text{kip}$$

Nominal yeild strength of a group anchors

4. Concrete Breakout Strength of Anchors in Tension, N_{cbg}

(ACI 318-19 Section 17.6.2)

$$\psi_1 := 1$$

Mod. Factor for eccentric loading

$$\psi_2 := 1$$

Mod. Factor for edge effects

$$\psi_3 := 1$$

Mod. Factor for uncracked concrete

$$\psi_4 := 1$$

Mod. Factor for breakout splitting

a. Projected Concrete Failure Area for Group Anchors, A_{nc}

$$A_{nc} := \left[1.5 \cdot h_{ef} + \left(n^{0.5} - 1 \right) \cdot s + 1.5 h_{ef} \right]^2 = 2450.25 \text{ in}^2 \quad \text{For Group Anchors}$$

b. Projected Concrete Failure Area of Single Anchor, A_{nc0}

$$A_{nc0} := 9 \cdot h_{ef}^2 = 1406.3 \text{ in}^2$$

c. Basic Single Anchor Breakout Strength, N_b

$$k_c := 31.4 \quad \text{For DWA, Extracted from previous tests}$$

$$N_b := \frac{k_c \cdot \lambda \cdot \sqrt{f'_c}}{1000 \cdot \sqrt{\text{psi}}} \cdot \left(\frac{h_{ef}}{\text{in}} \right)^{1.5} \cdot \text{kip} = 107.5 \cdot \text{kip}$$

d. Concrete Breakout Strength, N_{cbg}

The concrete breakout capacity as per ACI 318-19 for group anchors is given by equation 17.6.2.1b

$$N_{cbg} := \frac{A_{nc}}{A_{nc0}} \cdot \psi_1 \cdot \psi_2 \cdot \psi_3 \cdot \psi_4 \cdot N_b = 187.3 \cdot \text{kip}$$

e. Governing Failure

$$\left(\begin{array}{ll} \text{"Breakout failure"} & \text{if } N_{cbg} < N_s \\ \text{"Rebar Rupture"} & \text{otherwise} \end{array} \right) = \text{"Breakout failure"}$$

5. WELD STRENGTH

| | |
|--|--|
| $\theta := 90 \cdot \text{deg}$ | Angle between Axial Tensile force and weld |
| $F_{exx} := 70 \text{ksi}$ | |
| $F_y := 50 \text{ksi}$ | Nominal Yield Strength of Base Plate |
| $F_u := 65 \text{ksi}$ | |
| $a := 0.5 \text{in}$ | Throat of weld or size of weld |
| $t_p := 1.5 \text{in}$ | Thickness of Embed Plate |
| $F_{nw} := 0.6 \cdot F_{exx} \cdot 1.5 \cdot \sin(\theta)$ | |
| $F_{nw} = 63 \cdot \text{ksi}$ | |
| $R_u := 1.5 \cdot N_{cbg} = 280.937 \text{ kip}$ | |

1. Weld between Clevis Plates and Steel Ebdedment Plate

$$L_{cp} := 98 \text{ in}$$

$$L_{eff} := \begin{cases} L_{cp} & \text{if } L_{cp} \leq 100 \cdot a \\ (180 \cdot a) & \text{if } L_{cp} \geq 300 \cdot a \\ \left[L_{cp} \cdot \left(1.2 - 0.002 \cdot \frac{L_{cp}}{a} \right) \right] & \text{otherwise} \end{cases} = 79.18 \cdot \text{in}$$

$$L_{eff} = 79.184 \text{ in}$$

a. Weld Shear Strength, Rn_shear

$$\phi_{shear} := 0.75$$

$$R_{shear} := 0.707 \cdot a \cdot L_{eff} \cdot F_{nw} = 1763.47 \cdot \text{kip}$$

$$R_{n_shear} := \phi_{shear} \cdot R_{shear}$$

$$R_{n_shear} = 1322.6 \cdot \text{kip}$$

b. Base Metal Strength, Rn_base

(1) Nonimal Yeild Strength

$$\phi_y := 1$$

$$R_{n_yd} := \phi_y \cdot 0.6 \cdot F_y \cdot L_{eff} \cdot t_p$$

$$R_{n_yd} = 3563.28 \text{ kip}$$

(2) Nominal Rupture Strength

$$\phi_r := 0.75$$

$$Rn_r := \phi_r \cdot 0.6 \cdot Fu \cdot Leff \cdot tp$$

$$Rn_r = 3474.2 \text{ kip}$$

$$Rn_{base} := \min(Rn_{yd}, Rn_r)$$

$$Rn_{base} = 3474.2 \text{ kip}$$

c. Nonimal Shear Capacity, Rn

$$Rn := \min(Rn_{shear}, Rn_{base}) = 1322.6 \text{ kip}$$

d. Result

$$\begin{cases} \text{"Okay"} & \text{if } Rn \geq Ru \\ \text{"Revise"} & \text{otherwise} \end{cases} = \text{"Okay"}$$

2. Weld between Embedment Plates and Anchors (DWA)

$$a := 0.375 \text{ in}$$

Weld Size

$$L_{cp} := n \cdot 2 \cdot \pi \cdot \frac{db}{2} = 39.27 \text{ in}$$

$$L_{eff} := \begin{cases} L_{cp} & \text{if } L_{cp} \leq 100 \cdot a \\ (180 \cdot a) & \text{if } L_{cp} \geq 300 \cdot a \\ \left[L_{cp} \cdot \left(1.2 - 0.002 \cdot \frac{L_{cp}}{a} \right) \right] & \text{otherwise} \end{cases} = 38.9 \cdot \text{in}$$

$$L_{eff} = 38.899 \text{ in}$$

a. Weld Shear Strength, Rn_shear

$$\phi_{shear} := 0.75$$

$$R_{shear} := 0.707 \cdot a \cdot L_{eff} \cdot F_{nw} = 649.73 \cdot \text{kip}$$

$$R_{n_shear} := \phi_{shear} \cdot R_{shear}$$

$$R_{n_shear} = 487.3 \cdot \text{kip}$$

b. Base Metal Strength, Rn_base

(1) Nominal Yield Strength

$$\phi_y := 1$$

$$R_{n_yd} := \phi_y \cdot 0.6 \cdot F_y \cdot L_{eff} \cdot t_p$$

$$R_{n_yd} = 1750.46 \text{ kip}$$

(2) Nominal Rupture Strength

$$\phi_r := 0.75$$

$$Rn_r := \phi_r \cdot 0.6 \cdot Fu \cdot Leff \cdot tp$$

$$Rn_r = 1706.7 \text{ kip}$$

$$Rn_base := \min(Rn_yd, Rn_r)$$

$$Rn_base = 1706.7 \text{ kip}$$

c. Nonimal Shear Capacity, Rn

$$Rn := \min(Rn_shear, Rn_base) = 487.3 \text{ kip}$$

d. Result

$$\begin{cases} \text{"Okay"} & \text{if } Rn \geq Ru \\ \text{"Revise"} & \text{otherwise} \end{cases} = \text{"Okay"}$$

Design Example 2

Test # 6 5x5DWA $\frac{5}{8}$ ■

1. Data

$f'_c := 6000 \text{ psi}$ compressive strength of the concrete, psi

Steel Anchors Properties

Type DWA

$F_y := 70 \text{ ksi}$ Nominal Yield strength of bar

$d_b := 0.625 \text{ in}$ Dia of #5 DWA bar

$A_s := 0.3067 \text{ in}^2$ Area of #5 DWA bar

$n := 25$ Number of Anchors

$s := 3 \text{ in}$ Spacing between anchors (bars)

Steel Embedment Plate

$B := 15 \text{ in}$ Embed plate dimensions 15in x 15in

$L := 15 \text{ in}$

$t := 1.5 \text{ in}$ Embed plate thickness

2. Development Length, l_d

$\lambda := 1$ For normal weight concrete

$\psi_t := 1$ rebar location factor

$\psi_e := 1$ rebar coating factor

$\psi_s := 0.8$ rebar size factor (0.8 for bars less than #6)

-

$$C_{ktr} := 2.5$$

$$\frac{c + k_{tr}}{d_b} = 2.5$$

+

$$l_d := \left[\frac{3 \cdot F_y \cdot \psi_t \cdot \psi_e \cdot \psi_s}{40 \cdot \lambda \cdot (\sqrt{f_c \cdot \text{psi}}) \cdot C_{ktr}} \right] \cdot d_b$$

Development length for deformed bars or deformed wires per ACI 318-14 Section 25.4.2.3

$$l_d = 13.56 \text{ in}$$

$$h_f := l_d + t = 15.06 \text{ in}$$

Effective Anchor length including steel plate

$$h_{ef} := 15.5 \text{ in}$$

Rounding off to next 0.5

3. Nominal Steel Strength of Anchors in Tension, N_s (ACI 318-19 Section 17.6.1.2)

$$N_{sa} := A_s \cdot F_y = 21.469 \text{ kip}$$

Nominal yeild strength of a single anchor

$$N_s := n \cdot A_s \cdot F_y = 536.725 \text{ kip}$$

Nominal yeild strength of a group anchors

4. Concrete Breakout Strength of Anchors in Tension, N_{cbg}

(ACI 318-19 Section 17.6.2)

$$\psi_1 := 1$$

Mod. Factor for eccentric loading

$$\psi_2 := 1$$

Mod. Factor for edge effects

$$\psi_3 := 1$$

Mod. Factor for uncracked concrete

$$\psi_4 := 1$$

Mod. Factor for breakout splitting

a. Projected Concrete Failure Area for Group Anchors, Anc

$$Anc := \left[1.5 \cdot hef + \left(n^{0.5} - 1 \right) \cdot s + 1.5hef \right]^2 = 3422.25 \text{ in}^2 \quad \text{For Group Anchors}$$

b. Projected Concrete Failure Area of Single Anchor, Anco

$$Anco := 9 \cdot hef^2 = 2162.3 \text{ in}^2$$

c. Basic Single Anchor Breakout Strength, Nb

$$kc := 31.4 \quad \text{For DWA, Extracted from previous tests}$$

$$Nb := \frac{kc \cdot \lambda \cdot \sqrt{f_c}}{1000 \cdot \sqrt{\text{psi}}} \cdot \left(\frac{hef}{\text{in}} \right)^{1.5} \cdot \text{kip} = 148.4 \cdot \text{kip}$$

d. Concrete Breakout Strength, Ncbg

The concrete breakout capacity as per ACI 318-19 for group anchors is given by equation 17.6.2.1b

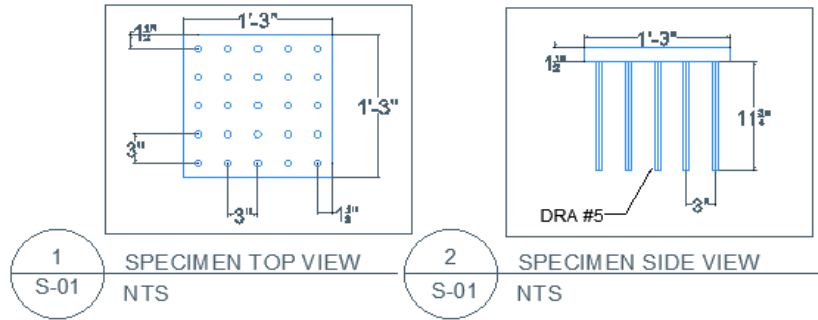
$$Ncbg := \frac{Anc}{Anco} \cdot \psi_1 \cdot \psi_2 \cdot \psi_3 \cdot \psi_4 \cdot Nb = 234.9 \cdot \text{kip}$$

e. Governing Failure

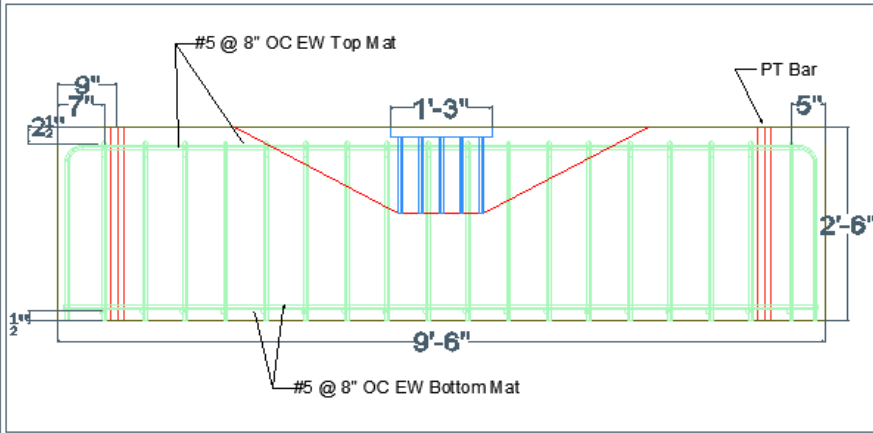
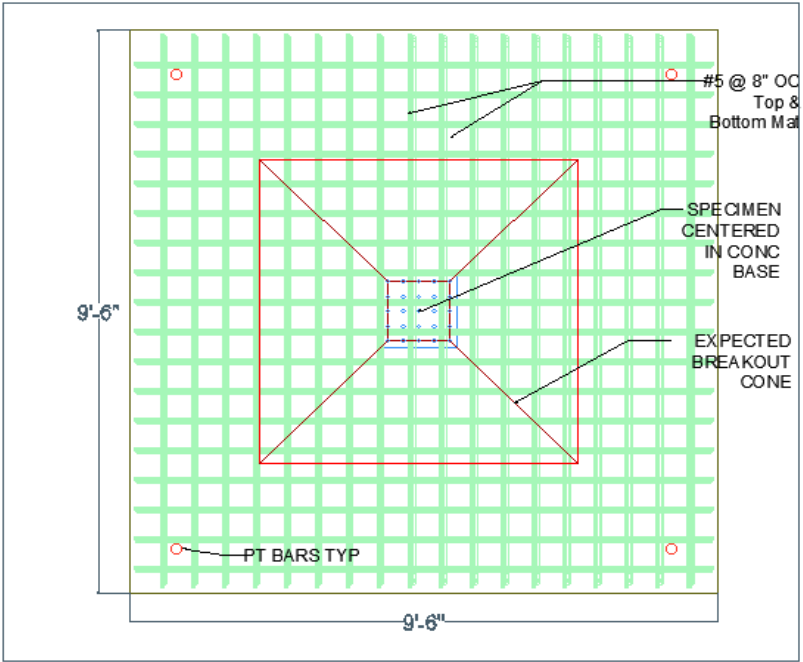
$$\left(\begin{array}{ll} \text{"Breakout failure"} & \text{if } Ncbg < Ns \\ \text{"Rebar Rupture"} & \text{otherwise} \end{array} \right) = \text{"Breakout failure"}$$

APPENDIX B

Group Anchor Specimen 1 and 2

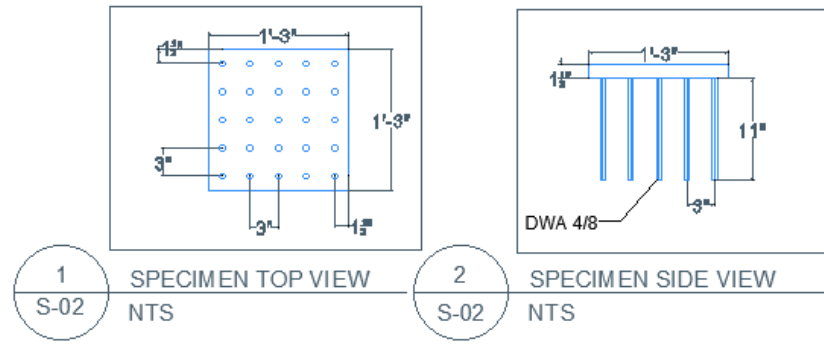


| ABBREVIATIONS: | |
|----------------|-----------------|
| CL | CENTERLINE |
| CONC | CONCRETE |
| NTS | NOT TO SCALE |
| OC | ON CENTER |
| PL | PLATE |
| PT | POST-TENSIONING |
| TYP | TYPICAL |

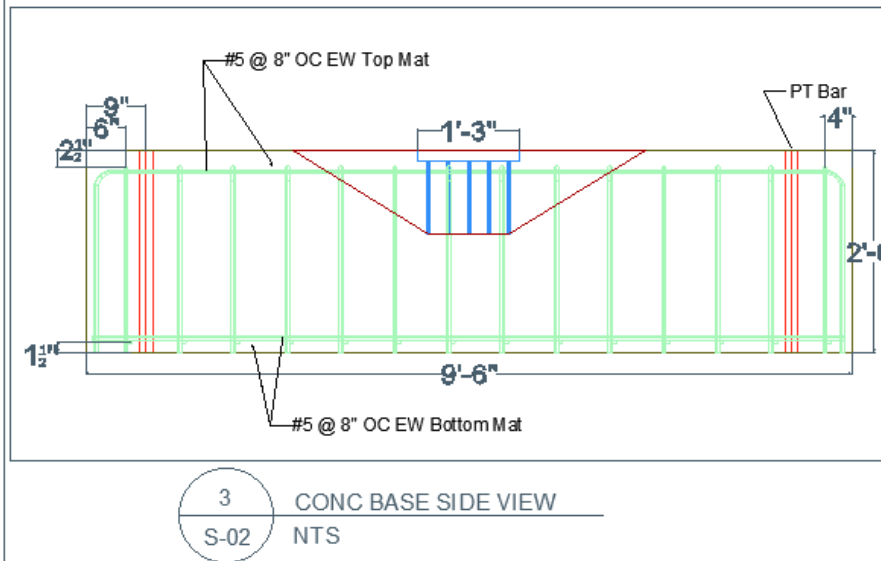
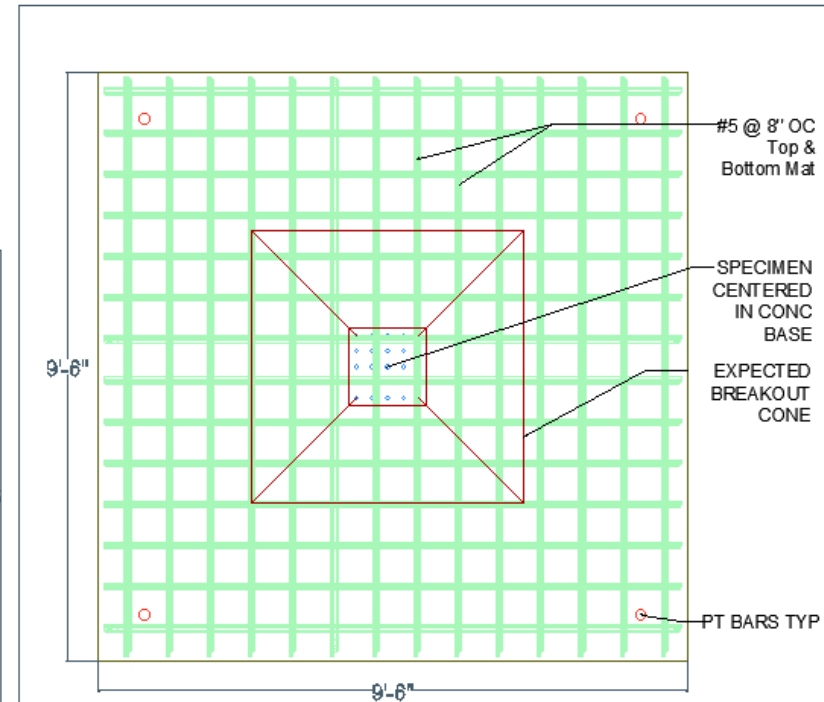


| | | | | | | |
|--------------|-------------------------------|----------|------------|-------------|------------|------|
| DRAWING NAME | GA Tests #1 and #2 | DRAWN BY | CHECKED BY | APPROVED BY | 12/08/2019 | S-01 |
| PROJECT NAME | KEPCO CONCRETE BREAKOUT TESTS | AUR | JS | AV | | |

Group Anchor Specimen 3 and 4

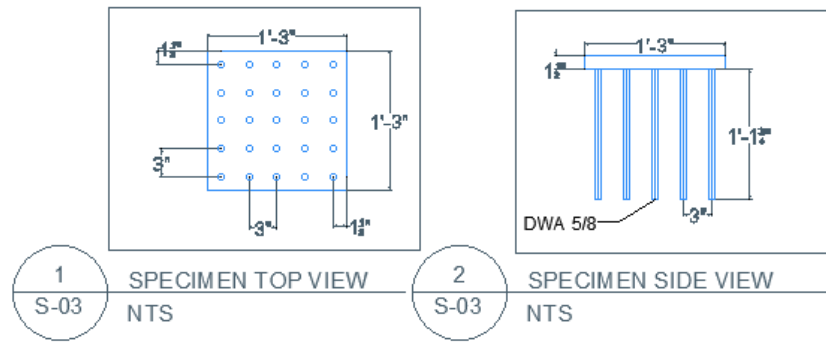


| ABBREVIATIONS: | |
|----------------|-----------------|
| CL | CENTERLINE |
| CONC | CONCRETE |
| NTS | NOT TO SCALE |
| OC | ON CENTER |
| PL | PLATE |
| PT | POST-TENSIONING |
| TYP | TYPICAL |

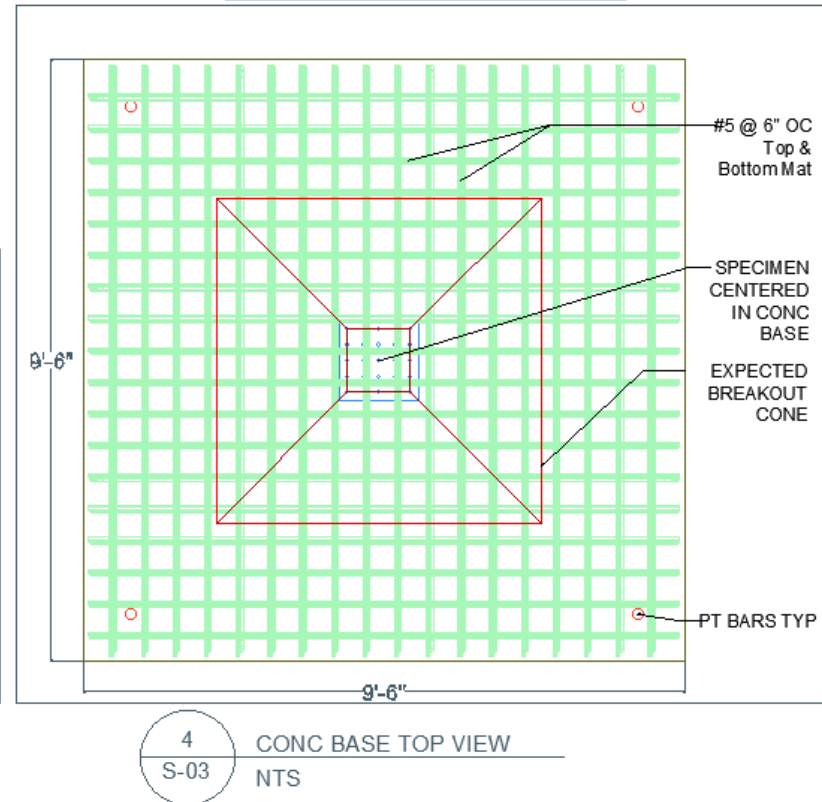
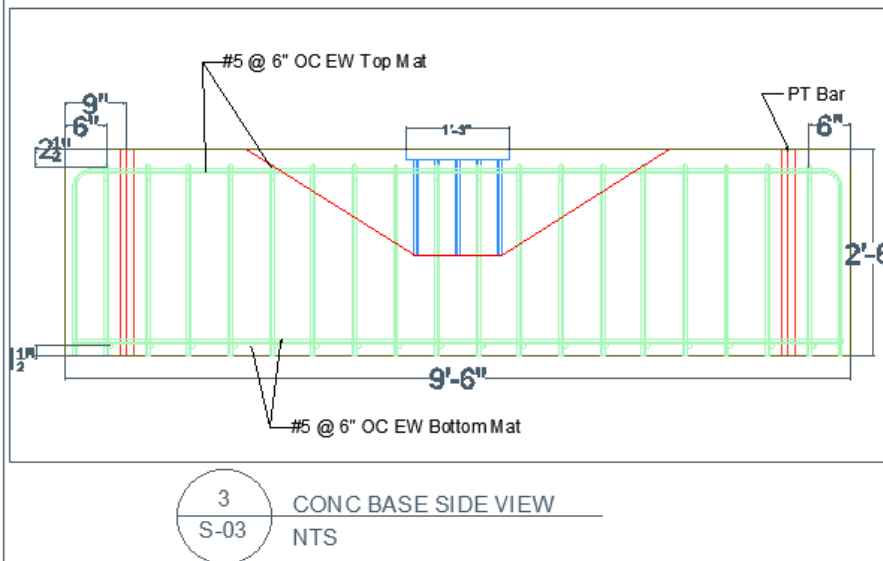


| | | | | | | |
|--------------|-------------------------------|----------|------------|-------------|-------------|------|
| DRAWING NAME | GA Tests #3 and #4 | DRAWN BY | CHECKED BY | APPROVED BY | 12/08/20 19 | S-02 |
| PROJECT NAME | KEPCO CONCRETE BREAKOUT TESTS | AUR | JS | AV | | |

Group Anchor Specimen 5 and 6

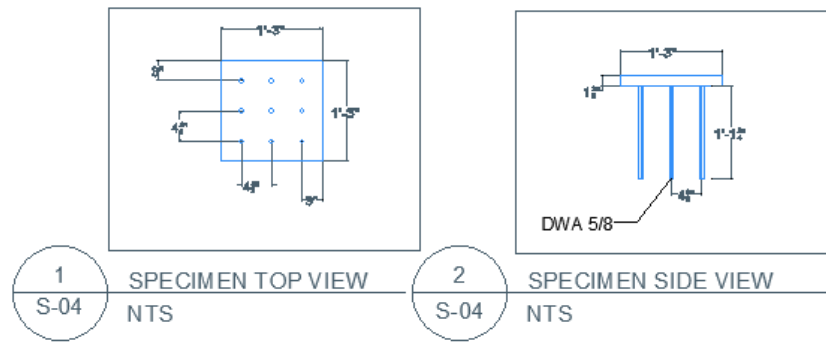


| ABBREVIATIONS: | |
|----------------|-----------------|
| CL | CENTERLINE |
| CONC | CONCRETE |
| NTS | NOT TO SCALE |
| OC | ON CENTER |
| PL | PLATE |
| PT | POST-TENSIONING |
| TYP | TYPICAL |

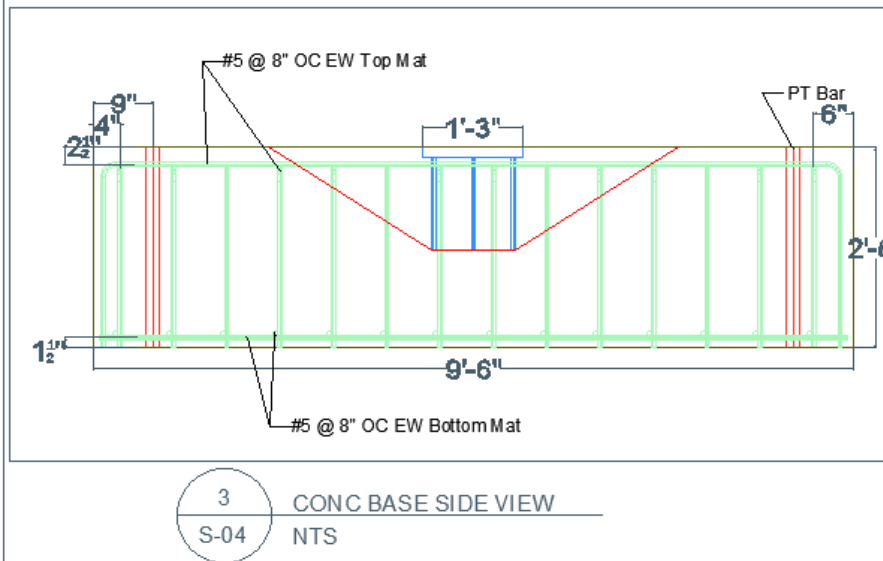
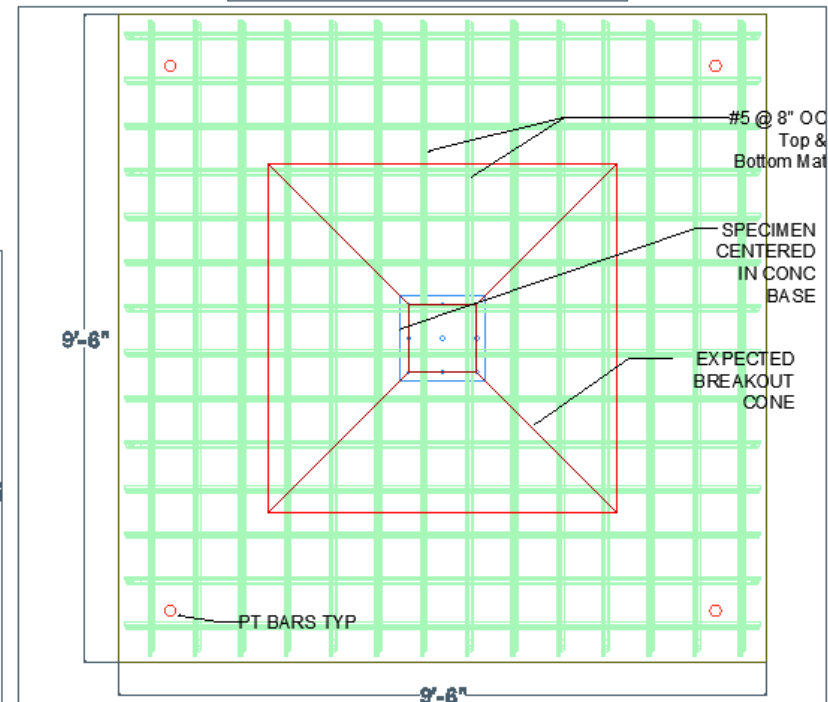


| | | | | | | |
|--------------|-------------------------------|----------|------------|-------------|------------|------|
| DRAWING NAME | GA Tests #5 and #6 | DRAWN BY | CHECKED BY | APPROVED BY | 12/08/2019 | S-03 |
| PROJECT NAME | KEPCO CONCRETE BREAKOUT TESTS | AUR | JS | AV | | |

Group Anchor Specimen 7

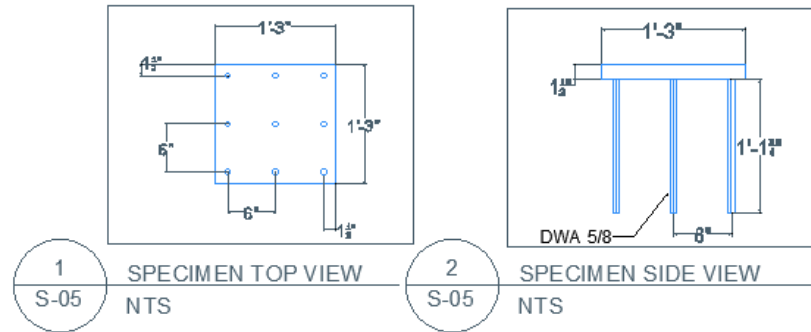


| ABBREVIATIONS: | |
|----------------|-----------------|
| CL | CENTERLINE |
| CONC | CONCRETE |
| NTS | NOT TO SCALE |
| OC | ON CENTER |
| PL | PLATE |
| PT | POST-TENSIONING |
| TYP | TYPICAL |

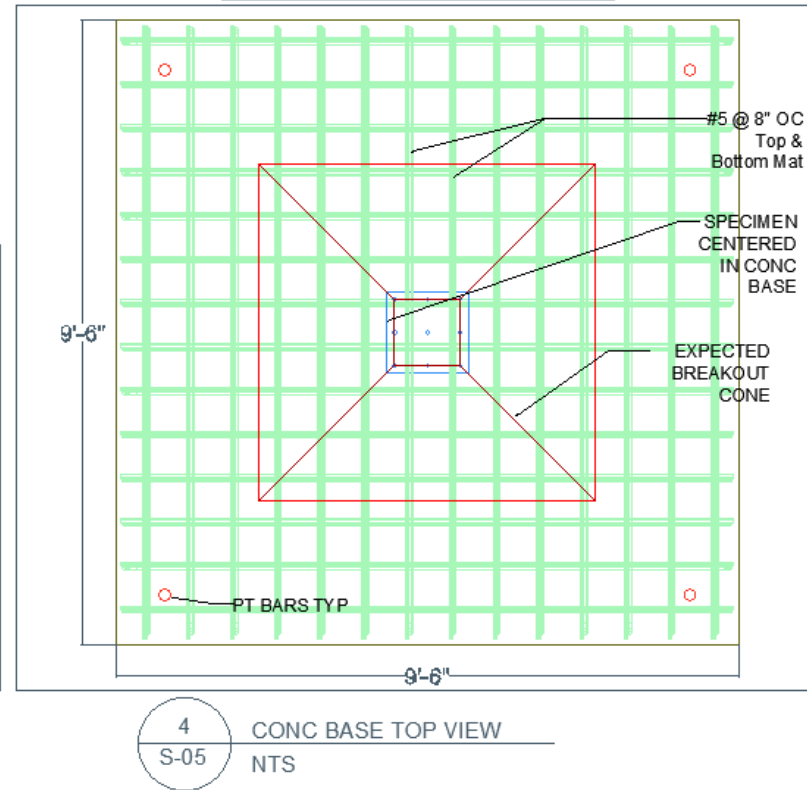
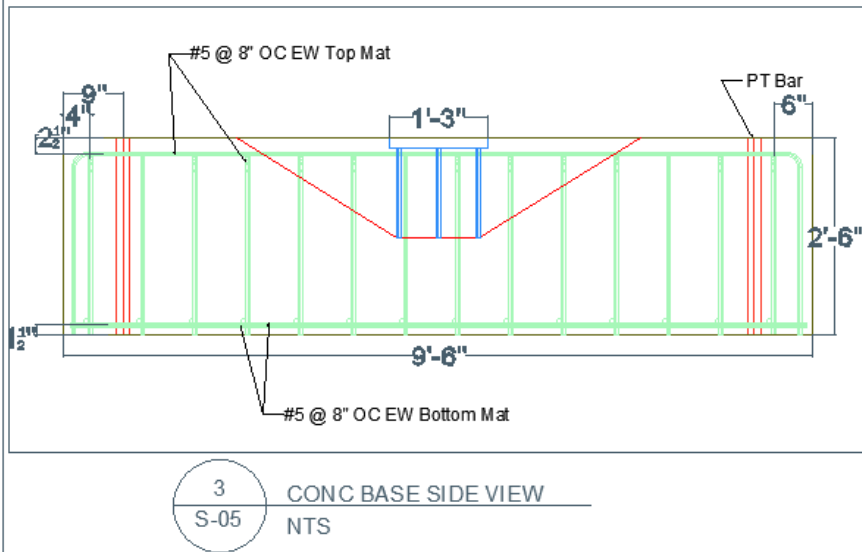


| | | | | | | |
|--------------|-------------------------------|----------|------------|-------------|------------|------|
| DRAWING NAME | GA Test #7 | DRAWN BY | CHECKED BY | APPROVED BY | 12/08/2019 | S-04 |
| PROJECT NAME | KEPCO CONCRETE BREAKOUT TESTS | AUR | JS | AV | | |

Group Anchor Specimen 8



| ABBREVIATIONS: | |
|----------------|-----------------|
| CL | CENTERLINE |
| CONC | CONCRETE |
| NTS | NOT TO SCALE |
| OC | ON CENTER |
| PL | PLATE |
| PT | POST-TENSIONING |
| TYP | TYPICAL |



73

| | | | | | | |
|--------------|-------------------------------|----------|------------|-------------|------------|------|
| DRAWING NAME | GA Test #8 | DRAWN BY | CHECKED BY | APPROVED BY | 12/08/2019 | S-05 |
| PROJECT NAME | KEPCO CONCRETE BREAKOUT TESTS | AUR | JS | AV | | |

APPENDIX C

Concrete Mix Design

| Material | | S.G. | Quantity (lb/yd ³) |
|--------------------|---------------------------|------|--------------------------------|
| Cement | Type 1 Cement (ASTM C150) | 3.15 | 548.4 |
| Fly Ash | Class F | 2.55 | 178.2 |
| Course Agg | #8 Limestone (INDOT) | 2.70 | 1664.6 |
| Fine Agg | Natural Sand | 2.65 | 1223.7 |
| Water | | 1.00 | 261.5 |
| Entrapped Air | | - | - |
| Water/Cement Ratio | | 0.36 | |